POWER DENSITY SPECTRA AND THEIR APPLICATION IN THE DETERMINATION OF AIRCRAFT GUST LOADS

By

LLOYD EARL JACKSON

Bachelor of Science

University of Tulsa

Tulsa, Oklahoma

1949

Submitted to the faculty of the Graduate School of
the Oklahoma State University
in partial fulfillment of the requirements
for the degree of
MASTER OF SCIENCE
August, 1961

POWER DENSITY SPECTRA AND THEIR APPLICATION

IN THE DETERMINATION OF

AIRCRAFT GUST LOADS

Thesis Approved:

Edwin J. Saller

Thesis Adviser

Roger L. Klanderman

Thesis Adviser

Dean of the Graduate School

ACKNOWLEDGEMENT

Sincere thanks is expressed to Professor Edwin J. Waller for the numerous hours of individual teaching he has afforded me during my graduate study.

I am very grateful, also, to Professor Jan J. Tuma for his untiring educational efforts and his positive approach in the encouragement of those in industry who seek to learn.

TABLE OF CONTENTS

LIST OF TABLES

LIST OF FIGURES

NOMENCLATURE

a_n	normal acceleration in units of g: coefficient of Fourier series
a_1, a_2, a_3	scale parameters in distribution $f(\sigma_{a_n})$
$\bar{A}$	σ_{a_n}/σ_u
b_n	coefficient of Fourier series
b_1	nonstorm turbulence scale factor in distribution $\hat{f}(\sigma_u)$
b_2	storm turbulence scale factor in distribution $\hat{f}(\sigma_u)$
D_i	flight distance in the i^{th} segment
c	structural damping coefficient
c_n	amplitude of alternating component
f(t)	arbitrary time function
$f(\sigma_{a_n})$	probability-density distribution of the root mean-square normal acceleration
$\hat{f}(\sigma_u)$	probability-density distribution of the root mean-square gust velocity
F_y	spring force acting in the lateral direction in pounds
F_z	spring force acting in the vertical direction in pounds
$F(i\omega)$	Fourier transform of f(t)
g	acceleration due to gravity, 386 inches per second^2
G_o	average number of response peaks per mile of flight
G(y)	average number of response peaks exceeding y (total of both positive and negative) per mile of flight

$G_t(y)$	expected number of response peaks exceeding given values of y
[G]	matrix of pylon influence coefficients, inches per pound
i	$\sqrt{-1}$
K_{ij}	term of [K] in the i^{th} row and the j^{th} column
[K]	matrix of pylon spring constants, pounds per inch
L	scale of turbulence in feet
M	mass in pounds seconds^2/inches
$\overline{M(a_n)}$	average number of positive acceleration peaks per second exceeding a_n
Δn	incremental load factor variation from mean value
n	interger; load factor in units of g
$N_o = \frac{1}{2\pi}\left[\frac{\int_o^\infty \omega^2 \Phi(\omega)\,d\omega}{\int_o^\infty \Phi(\omega)\,d\omega}\right]^{1/2}$	with ω in radians/sec.
$N(a_n)$	average number of maximum accelerations per second exceeding a_n
$p_1(v_1,t_1)$	first probability-density distribution for an ensemble of signals v(t)
$p_2(v_1,t_1;v_2,t_2)$	second probability-density distribution for ensemble of signals v(t)
$p_1(v_1)$	first probability-density distribution of a stationary stochastic signal v(t)
$p_2(v_1,v_2,\tau)$	second probability-density distribution of a stationary stochastic signal v(t)
$P_1(a<v_1<b)$	first probability function of v(t)
$P_2(a<v_1<b, c<v_2<d)$	second probability function of v(t)

P_1	proportion of total flight distance in nonstorm turbulence
P_2	proportion of total flight distance in storm turbulence
P_i	proportion of the total flight in the i^{th} condition
$q(t)$	output or response function
$Q(i\omega)$	Fourier transform of $q(t)$
t	time
T	arbitrary value of time; period of $f(t)$
$v(t)$	arbitrary input function
V	velocity in feet/second
$V(i\omega)$	Fourier transform of $v(t)$
$w(t)$	weighting function
$W(i\omega)$	system transfer function with respect to the frequency argument ω
$W(i\Omega)$	system transfer function with respect to the frequency argument Ω
$\lvert W(i\omega) \rvert$	modulus of complex function $W(i\omega)$
x	displacement
y	lateral displacement in inches; any desired response parameter
$\ddot{y} = d^2y/dt^2$	
$Y(i\omega)$	Fourier transform of $y(t)$
$Y'(i\omega)$	pylon transfer function in the lateral direction for a vertical input
z	vertical displacement in inches
$\ddot{z} = d^2z/dt^2$	
$Z(i\omega)$	Fourier transform of $z(t)$

$Z(i\omega)$	pylon transfer function in the vertical direction for a vertical input
a_n	complex coefficient of Fourier series
λ	$\omega^2/(1 + ic)$
σ	standard deviation of Gaussian distribution
σ_{a_n}	root mean-square acceleration in feet/second^2
σ_u	root mean-square gust velocity in feet/second
τ	time displacement
$\phi_{qq}(\tau)$	autocorrelation function of q(t)
$\phi_{vv}(\tau)$	autocorrelation function of v(t)
$\phi_{vu}(\tau)$	cross-correlation function of v(t) and u(t)
$\Phi_{qq}(i\omega)$	power density spectrum of q(t)
$\Phi_{vv}(i\omega)$	power density spectrum of v(t)
$\Phi_{a_n}(\omega)$	power density spectrum of normal acceleration in g^2/(radians/sec.^{2})
$\Phi_i(\omega)$	power density spectrum of input function at pylon to wing attachment in g^2/cps
$\Phi_{o_{y_o}}(\omega)$	power density spectrum of output function in the lateral direction at the c.g. of the outboard store in g^2/cps
$\Phi_{o_{z_o}}(\omega)$	power density spectrum of output function in the vertical direction at the c.g. of the outboard store in g^2/cps
$\Phi(\Omega)$	power density spectrum of an arbitrary function with respect to the frequency argument Ω.
$\Phi_{a_n}(\Omega)$	power density spectrum of normal acceleration in (g^2)/(radians/foot)
$\Phi_u(\Omega)$	power density spectrum of gust velocity in (feet/second)^2/(radians/foot)

Ψ_n	relative phase angle of harmonic component
ω	angular frequency in radains/second unless otherwise noted
Ω	reduced frequency, ω/V, in radians/foot
Subscripts	i - inboard o - outboard y - lateral z - vertical
$\overline{\quad}$	a bar over a symbol designates the time average value of the quantity
$\sim\!\!\sim$	a wiggle bar over a symbol designates the ensemble average value of the quantity

INTRODUCTION

In recent years, the use of power density spectra for the prediction of aircraft gust loads has been extensively studied and developed into a practical engineering tool. Its primary value is in predicting the cyclic loads imposed on aircraft structures for use in evaluating their structural fatigue life. Thus, in this application power density spectra are important primarily to the structural engineer and yet are based on principles far more familiar to the automatic control system engineer and the dynamics engineer.

If the structural engineer is to derive cyclic load data or even properly interpret and make use of load data derived from power spectral density analyses, it is considered essential that he have a firm basic understanding of the method. This has prompted the author's interest in the subject.

The basic fundamentals involved in defining the response of a linear system to a stochastic input are discussed in Chapter I. The published power spectral density methods for the prediction of aircraft gust loads are set forth in Chapter II. The intent of these chapters is to bring together pieces from numerous references in such a way that the reader can establish the necessary background for application of the method.

In Chapter III a prediction of cyclic load due to an atmospheric turbulence condition is developed for a wing mounted pylon carrying dual high mass stores. The purpose of this analysis is to investigage the structural significance of considering the transfer functions of the pylon structure itself in developing these cyclic loads from a known power density spectrum of acceleration input at the pylon to wing attachment point. The usual engineering practime in fatigue load studies has been to consider this effect of pylon flexibility as secondary and, therefore, assume that the accelerations felt by the supported store are the same as the input to the pylon.

A procedure is developed for calculating the pylon transfer functions from stress analysis data which defines the pylon deflection influence coefficients. These functions are then used to obtain the power density spectra of output accelerations at the center of gravity of a supported store. The corresponding prediction of the frequency of occurence of these accelerations is obtained by methods discussed in Chapter II.

This investigation shows that the fatigue loading predicted by considering the pylon transfer functions can be considerably more severe than that predicted directly from the input spectrum. In the example investigated, a vertical acceleration input only is considered; however, the power spectral density analysis reveals an induced lateral acceleration at the center of gravity of the supported stores. This

occurs at a pylon/store system resonant frequency and accounts for the major portion of the increased severity of the predicted fatigue loading.

CHAPTER I

LINEAR SYSTEM RESPONSE TO A STOCHASTIC INPUT

1.1 Discussion

The output of a linear system subjected to a unique input function may be specifically defined by solving the applicable integro-differential equations. Solution of these equations may be accomplished in the time[1] domain, or in the frequency domain by the use of Fourier or Laplace transforms where applicable.

The output of a linear system subjected to a stochastic input function, one which contains a degree of randomness, cannot be solved for in terms of specific and unique values as a function of time; however, it can be defined in terms of probability distributions. The solution may be accomplished in the time domain making use of correlation functions, or in the frequency domain by the use of power density spectra which are obtained by Fourier transformation of the correlation functions.

It is desirable to discuss first some of the fundamentals of linear system analysis, Fourier transforms, procedures

---

[1]Time is considered herein as the independent variable; however, the statements and procedures of this chapter are applicable to any independent variable.

applicable to the frequency domain, and stochastic processes. This will provide background information for then proceeding with the discussion of the power spectral density analysis of linear systems subjected to a stochastic input.

1.2 Weighting Function

A linear system is one for which the principle of superposition holds true. That is, if the system is acted upon by several inputs simultaneously, its output will equal the sum of the outputs from the individual inputs applied independently. This property is of prime importance in simplifying the solution of problems involving linear systems.

The unit impulse function can be defined as the limit of a rectangular pulse whose amplitude approaches infinity as its width approaches zero with the area maintained equal to one unit of time. (1)[2] This is indicated in Fig. 1.

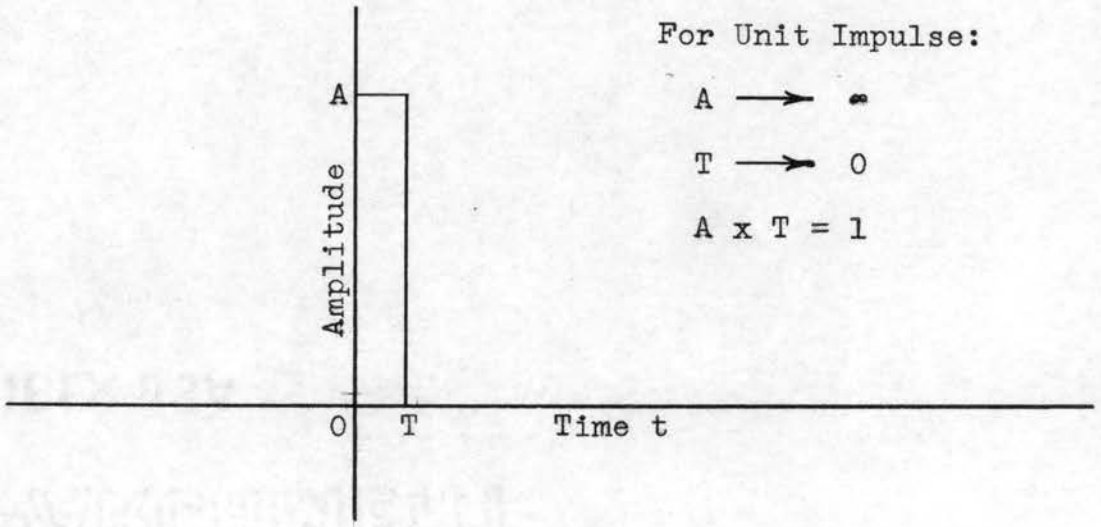

Fig. 1 - Unit Impulse Function

[2] A parenthesized number within the text, refers to the correspondingly numbered reference in the Bibliography, if not otherwise defined.

The response of a linear system to a unit impulse function is a unique characteristic of that system. The function which defines this response is known as the system weighting function, w(t). An example is shown in Fig. 2.

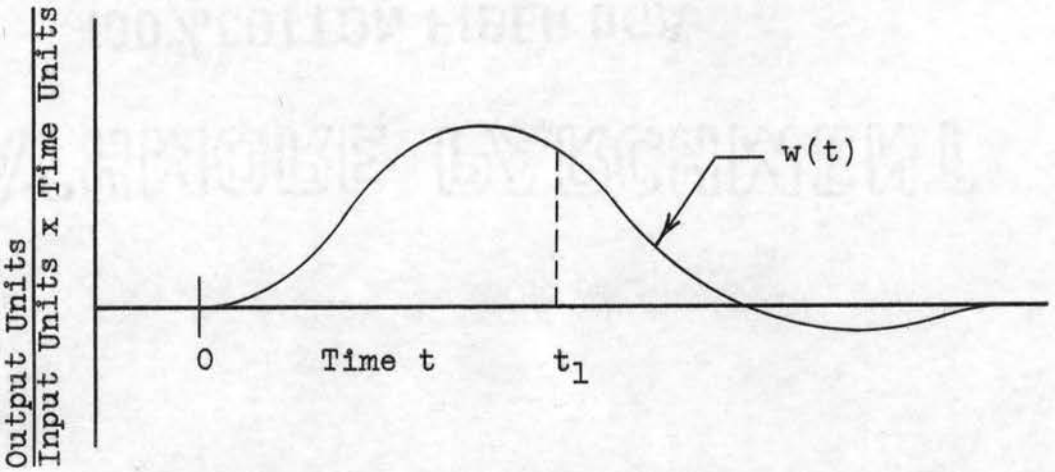

Fig. 2 - Example of System Weighting Function

It should be recognized that for any physically realizable system the system weighting function is equal to zero for negative time; in other words an effect cannot precede its cause.

If the input impulse strength is greater than unity, as defined by the area beneath it, the linear system output is proportionately greater than the unit impulse output. Thus if the curve of Fig. 3 were considered the input and the curve of Fig. 2 the system weighting function, the output at time t due to the shaded input impulse of Fig. 3, t_1 seconds earlier, would be

$$\Delta q(t) = w(t_1)v(t-t_1)\Delta t_1, \tag{1}$$

$$dq(t) = w(t_1)v(t-t_1)dt_1. \tag{2}$$

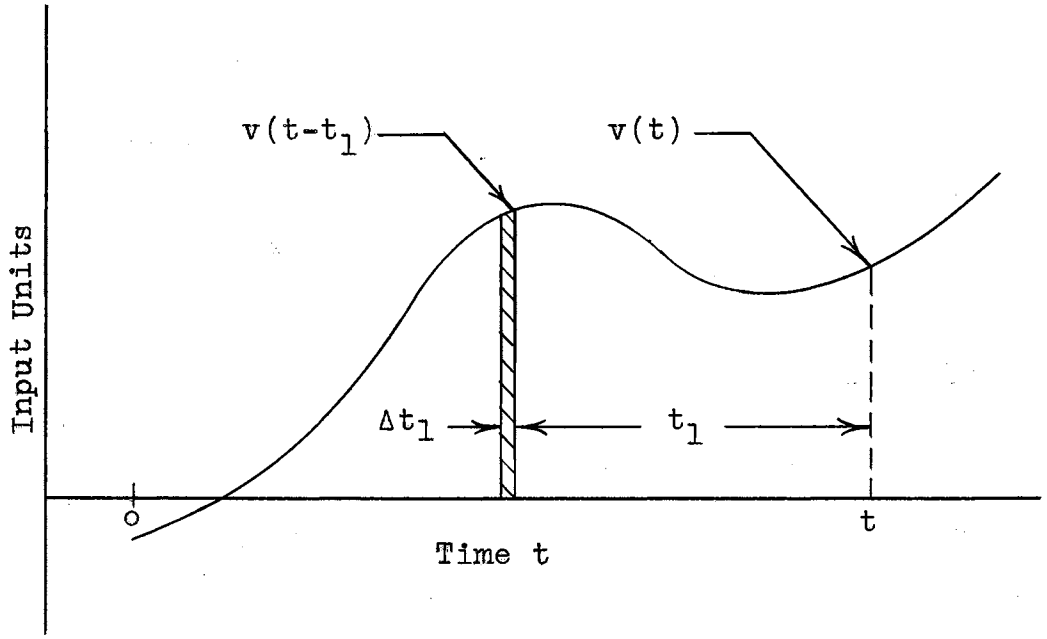

Fig. 3 - Input Function

By superposition of the output of all the incremental input impulses, the total output is given by equation (3).

$$q(t) = \int_{-\infty}^{\infty} w(t_1)v(t-t_1)dt_1. \qquad (3)$$

The right side of equation (3) is known as the convolution integral.

1.3 Fourier Series, Fourier Integral, and Fourier Transform

A periodic function, f(t), may be expanded into a Fourier series if it satisfies the Dirichlet conditions, which are:

1. The function has at most a finite number of discontinuities in one period.
2. The function has at most a finite number of maxima and minima in one period.
3. The integral $\int_{-T/2}^{T/2} f(t)\,dt$ is finite. (2)

By expansion into a Fourier series, the function f(t) is defined in harmonic sinusoidal components. This permits arbitrary waveforms to be expressed in terms of their amplitude spectra, or frequency spectra as they are more commonly termed. The response of a linear system to the input function, f(t), may then be determined by superposition of its responses to the various frequency components of the input function.(2)

The Fourier series expansion of f(t) is

$$f(t)=\frac{a_o}{2}+\sum_{n=1}^{\infty}(a_n \cos n\omega t + b_n \sin n\omega t), \qquad (4)$$

with

$$a_n = \frac{2}{T}\int_{-T/2}^{T/2} f(t) \cos n\omega t \, dt, \qquad (n=0,1,2,\ldots) \qquad (5)$$

$$b_n = \frac{2}{T}\int_{-T/2}^{T/2} f(t) \sin n\omega t \, dt, \qquad (n=1,2,3,\ldots) \qquad (6)$$

where

T = period of f(t),

$\omega = 2\pi/T$, angular frequency.

Another form of equation (4) is

$$f(t)=\frac{a_o}{2}+\sum_{n=1}^{\infty} c_n \cos (n\omega t-\Psi_n), \qquad (7)$$

where

$$c_n = \sqrt{a_n^2 + b_n^2}, \qquad (8)$$

$$\Psi_n = \tan^{-1} (b_n/a_n). \qquad (9)$$

The value of c_n represents the amplitude of the alternating component of f(t) which adds to the constant component, $a_o/2$. This amplitude, c_n, takes on a specific value for each

specific harmonic frequency $n\omega$. The angle Ψ_n is the relative phase of the harmonic components. It is also a function of $n\omega$ taking on specific values for each integral value of $n\omega$.

A plot of $|c_n|$ versus $n\omega$ is called the frequency spectrum of $f(t)$. Actually $|c_n|$ has values only at integral values of $n\omega$, so the frequency spectrum for a periodic function is really a series of line graphs as shown by the example in Fig. 4. It can be seen, however, that as the period T increases and ω, which is $2\pi/T$, decreases, the lines will be closer together and in the limit as $T \to \infty$, a smooth curve will result; this is the case for a nonperiodic function $f(t)$.

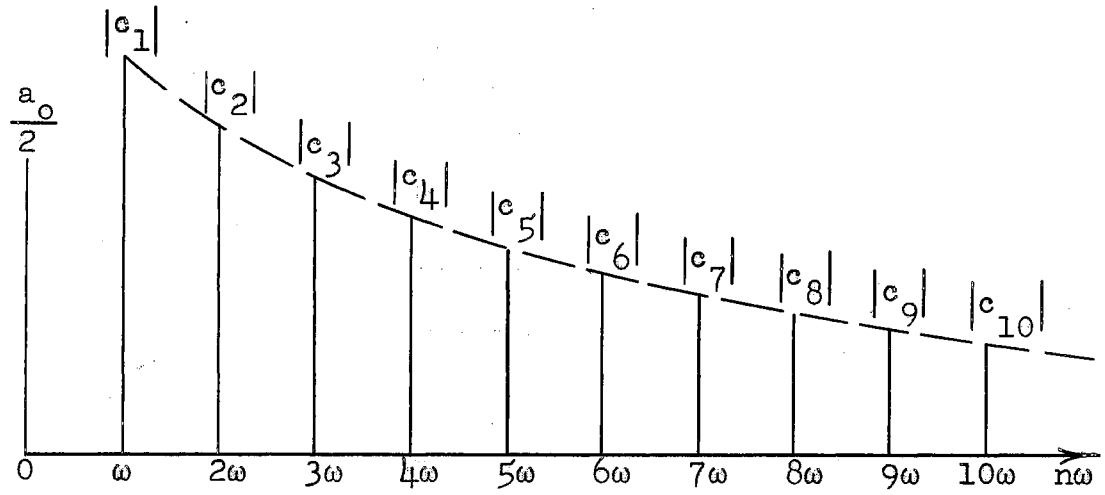

Fig. 4 - Frequency Spectrum of $f(t)$

In order to visualize the basis for the Fourier integral which is applicable to nonperiodic functions, it is helpful to express equation (4), for periodic functions, in exponential form. Since, by the familiar Euler's relation,

$$\left.\begin{aligned} \sin n\omega t &= \frac{e^{i\omega t} - e^{-i\omega t}}{2i} \\ \text{and} \\ \cos n\omega t &= \frac{e^{i\omega t} + e^{-i\omega t}}{2}, \end{aligned}\right\} \quad (10)$$

equation (4) can be reduced to

$$f(t) = \sum_{n=-\infty}^{\infty} a_n e^{in\omega t}, \quad (11)$$

where

$$a_n = \frac{1}{T}\int_{-T/2}^{T/2} f(t)e^{-in\omega t}dt. \quad (12)$$

In this case a_n is a complex coefficient. It can be shown that

$$2|a_n| = |c_n| \text{ of equation (8)}, \quad (13)$$

so a plot of $2|a_n|$ versus $n\omega$ would be the frequency spectrum of $f(t)$.

A nonperiodic function, $f(t)$, may be expressed as a Fourier integral which develops directly from equations (11) and (12). For a nonperiodic function, $T \to \infty$ and ω (which is $2\pi/T$) approaches an infinitesimally small value, $d\omega$, while n becomes meaningless. Thus, the Fourier integral for $f(t)$ is given by equation (14).

$$f(t) = \frac{1}{2\pi}\int_{-\infty}^{\infty}\left[\int_{-\infty}^{\infty} f(t)e^{-i\omega t}dt\right]e^{i\omega t}d\omega. \quad (14)$$

The Fourier integral is made up of what are termed the Fourier transform pairs:

The Fourier transform of $f(t)$ is

$$F(i\omega) = \int_{-\infty}^{\infty} f(t)e^{-i\omega t}dt. \quad (15)$$

This transformation produces a function in the frequency, ω, domain.

The inverse Fourier transform of $F(i\omega)$ is

$$f(t) = \frac{1}{2\pi} \int_{-\infty}^{\infty} F(i\omega) e^{i\omega t} d\omega. \tag{16}$$

This converts the frequency domain equation back to the time domain.

As stated by Cheng (2), $f(t)$ may be regarded as being analyzed into an infinite number of frequency components with infinitesimal amplitude $(1/2\pi)\ F(i\omega)\ d\omega$. A plot of $\left|F(i\omega)\right|$ versus ω shows the relative frequency distribution of $f(t)$.

In order for a nonperiodic function, $f(t)$, to be expressible as a Fourier integral or to be Fourier transformable, it must meet the Dirichlet conditions and the convergence condition as follows:

1. Function $f(t)$ can have only a finite number of discontinuities in the finite interval $t_1<t<t_2$.
2. Function $f(t)$ can have only a finite number of points at which the function becomes infinite in the finite interval $t_1<t<t_2$.
3. Function $f(t)$ can have only a finite number of maxima and minima in any finite interval $t_1<t<t_2$.
4. The integral $\int_{-\infty}^{\infty} f(t)\ dt$ must be finite.[2]

---

[2] This condition is arbitrarily complied with in dealing with continuous disturbances by ignoring the true values of $f(t)$ outside of the time range of interest and assuming there that $f(t) = 0$.

1.4 System Transfer Function

The analysis of a linear system may be accomplished in the frequency domain. The frequency domain equation corresponding to equation (3) may be obtained by Fourier transformation of both sides of equation (3).

$$\int_{-\infty}^{\infty} e^{-i\omega t} q(t)dt = \int_{-\infty}^{\infty} e^{-i\omega t} dt \int_{-\infty}^{\infty} w(t_1)v(t-t_1)dt_1. \qquad (17)$$

By interchanging the order of integration on the right side of equation (17),

$$Q(i\omega) = \int_{-\infty}^{\infty} w(t_1)dt_1 \int_{-\infty}^{\infty} e^{-i\omega t} v(t-t_1)dt. \qquad (18)$$

The variable of integration of the integral on the right is changed from t to $(t-t_1)$, then

$$Q(i\omega) = \int_{-\infty}^{\infty} e^{-i\omega t_1} w(t_1)dt_1 \int_{-\infty}^{\infty} e^{-i\omega(t-t_1)} v(t-t_1)d(t-t_1). \qquad (19)$$

Now dealing with the right side of equation (19), the integral on the right is the Fourier transform of the input, or $V(i\omega)$; the other integral is the Fourier transform of the weighting function, or $W(i\omega)$. Therefore, in the frequency domain

$$Q(i\omega) = W(i\omega)V(i\omega). \qquad (20)$$

Equation (20) is the frequency domain equivalent of the convolution integral, equation (3).

$W(i\omega)$ is known as the system transfer function.

1.5 Stochastic Processes

A Stochastic Process is one in which there is an element of chance. It is not necessarily purely random but contains a degree of randomness.

Whereas the value of a predictable function can be defined specifically as a function of time, the value of a stochastic function at a future time can be defined only in terms of the probability of its lying in a specified range.(1)

An ensemble of a stochastic signals is displayed in Fig. 5. Each record displays the signal from a specific machine. Identical types of machines have produced the ensemble of signals.

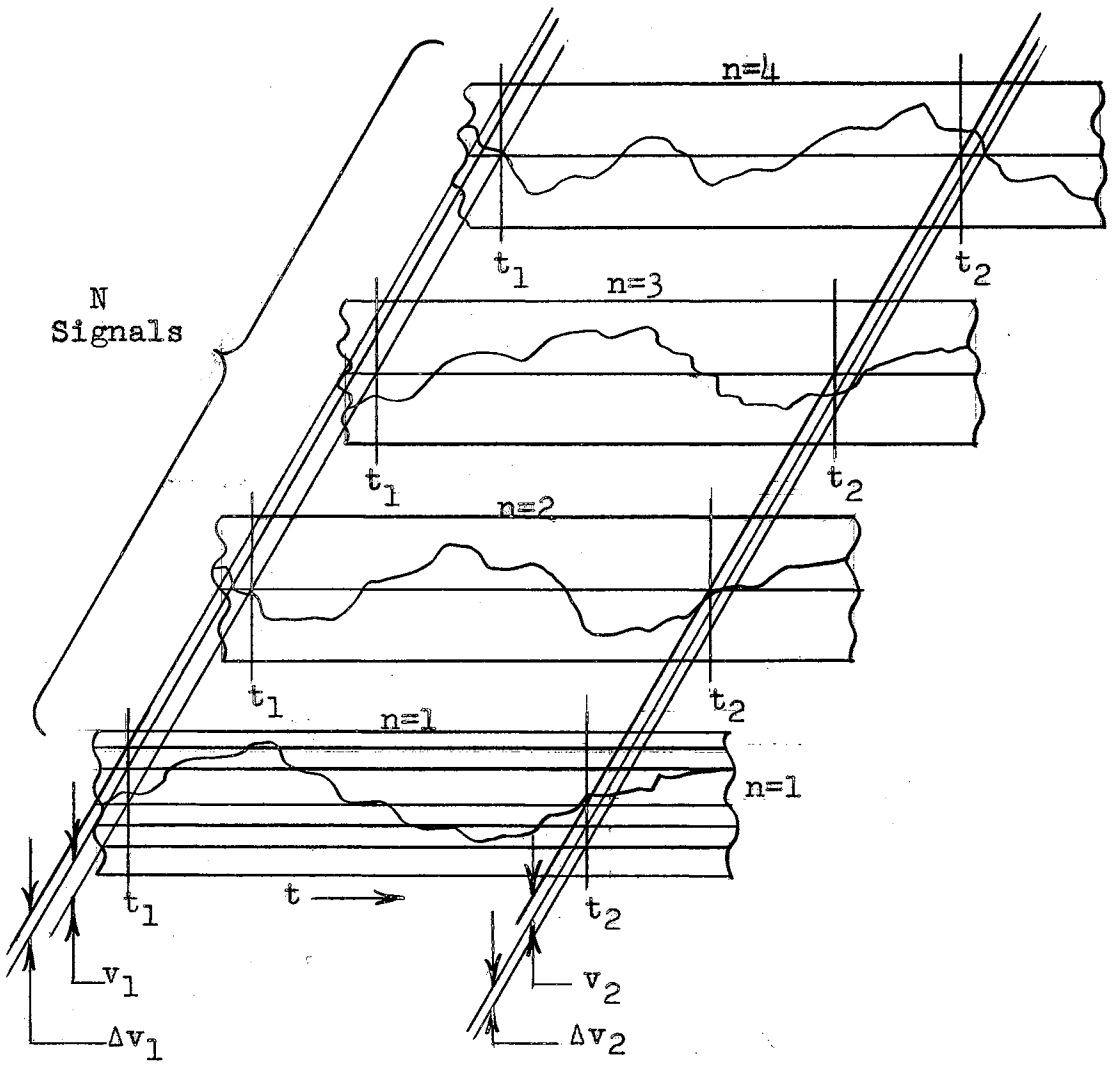

Fig. 5 - Ensemble of Stochastic Signals

The first probability density distribution function for this ensemble is determined from equation (21),

$$p_1(v_1,t_1) = \lim_{\substack{N\to\infty \\ \Delta v_1 \to 0}} \frac{\dfrac{[\Delta N_1(v_1,t_1,\Delta v_1;N)]}{N}}{\Delta v_1}, \tag{21}$$

where

N = total number of signals in the ensemble

$\Delta N_1(v_1,t_1,\Delta v_1;N)$ = number of signals lying between v_1 and $v_1+\Delta v_1$ at time t_1.

The probability of a signal lying between v_1 and v_1+dv_1 at t_1 is $p_1(v_1,t_1)dv_1$. Thus the probability of v_1 having a value between a and b at time t_1 is

$$P_1(a<v_1<b) = \int_a^b p_1(v_1,t_1)dv_1. \tag{22}$$

It follows that

$$P_1(-\infty<v_1<\infty) = \int_{-\infty}^{\infty} p_1(v_1,t_1)dv_1 = 1. \tag{23}$$

The ensemble average value of v_1 at t_1 is

$$v(t_1) = \int_{-\infty}^{\infty} v_1\, p_1(v_1,t_1)dv_1. \tag{24}$$

The second probability density distribution function is determined from equation (25)

$$p_2(v_1,t_1;v_2,t_2) = \lim_{\substack{N\to\infty \\ \Delta v_1 \to 0 \\ \Delta v_2 \to 0}} \frac{\dfrac{[\Delta N_2(v_1,t_1,\Delta v_1;v_2,t_2,\Delta v_2;N)]}{N}}{\Delta v_1\, \Delta v_2}, \tag{25}$$

where

$\Delta N_2(v_1,t_1,\Delta v_1;v_2,t_2,\Delta v_2;N)$ = number of signals lying between v_1 and $v_1+\Delta v_1$, at time t_1 and also lying between v_2 and $v_2+\Delta v_2$ at time t_2.

The probability of v_1 having a value between a and b at time t_1 and v_2 having a value between c and d at time t_2 is

$$P_2(a<v_1<b, c<v_2<d) = \int_a^b dv_1 \int_c^d p_2(v_1,t_1;v_2,t_2)dv_2. \quad (26)$$

By procedures similar to equation (21) and (25), the 3rd, 4th, ... nth probability-density distribution may be developed. It is by means of these probability-density distribution functions that the complete statistical characteristics of a stochastic process may be defined.

A non-stationary stochastic process is characterized by probability-density distributions which vary with time. If the probability-density distributions are independent of time the stochastic process is termed stationary. In this latter case, regardless of where t_1 is chosen in Fig. 5, the value of the first probability-density distribution remains constant and the value of the second probability-density distribution is also a constant for a given t_2-t_1, or τ, etc. The definition of the statistical characteristics is thus simplified.

It would appear, for a stationary process, that it is possible to define the statistics of the stochastic signal by using only one record of infinite length rather than the ensemble. This assumption, which is generally accepted and

successfully used is termed the ergodic hypothesis.(1) The first probability-density distribution is then determined by equation (27).

$$p_1(v_1) = \lim_{\substack{T\to\infty \\ \Delta v_1 \to 0}} \frac{\dfrac{[\Delta T_1(v_1, \Delta v_1, T)]}{T}}{\Delta v_1}, \tag{27}$$

where

T = total time range through which the time t_1 for signal value v_1 is swept.

$\Delta T_1(v_1, \Delta v_1, T)$ = total time during which the signal at time t_1 lies between v_1 and $v_1+\Delta v_1$, as t_1 moves through T.

Obviously T cannot be infinite. As a result of the Strong law of large numbers, the complete statistical characteristics can be defined by using a record of finite time length; however, confidence in the validity of the statistical description will increase proportionately as T increases. (3)

The second probability-density distribution for a stationary stochastic process is determined from a single record or time history by equation (28).

$$p_2(v_1, v_2, \tau) = \lim_{\substack{T\to\infty \\ \Delta v_1 \to 0 \\ \Delta v_2 \to 0}} \frac{\dfrac{[\Delta T_2(v_1, \Delta v_1, \tau_1, v_2, \Delta v_2, T)]}{T}}{\Delta v_1 \, \Delta v_2}, \tag{28}$$

where

$\Delta T_2(v_1,\Delta v_1,\tau_1,v_2,\Delta v_2,T)$ = total time during which the signal at time t_1 lies between v_1 and $v_1+\Delta v_1$ and also at time $t_2 = t_1+\tau$ lies between v_2 and $v_2+\Delta v_2$ as t_1 moves through T.

1.6 Correlation Functions

Correlation functions are used in the analysis of stochastic processes whether the analysis is carried out in the time domain or the frequency domain. They are related to the second probability-density distribution just discussed.

The autocorrelation function is defined as the ensemble average of the product of the signal at time t_1 and the signal at time t_2 or $t_1+\tau$ as indicated in equation (29)

$$\phi_{vv}(t_1,\tau) = \widetilde{v(t_1)v(t_1+\tau)}\ , \tag{29}$$

where

$\phi_{vv}(t_1,\tau)$ = the autocorrelation function of v(t).

The second probability density distribution function may be used to determine the autocorrelation function:

$$\phi_{vv}(t_1,\tau) = \int_{-\infty}^{\infty} v_1 dv_1 \int_{-\infty}^{\infty} v_2 p_2(v_1,t_1;v_2,t_1+\tau)dv_2. \tag{30}$$

It characterizes the signal but is not uniquely associated with the signal; i.e., a specific signal has a specific autocorrelation function, but an autocorrelation function cannot be analyzed to determine the specific signal from which it was derived.

In the case of a stationary stochastic process, the autocorrelation function can be defined as the time average of the

product of the signal at time t_1 and the signal at time $t_1+\tau$ in accordance with the ergodic hypothesis. Thus

$$\phi_{vv}(\tau) = \overline{v(t)v(t+\tau)}, \tag{31}$$

or

$$\phi_{vv}(\tau) = \lim_{T\to\infty} \frac{1}{2T} \int_{-T}^{T} v(t)v(t+\tau)dt. \tag{32}$$

For the stationary case the value of $\phi_{vv}(\tau)$ is unchanged whether τ is plus or minus, thus,

$$\phi_{vv}(\tau) = \phi_{vv}(-\tau); \tag{33}$$

i.e., the autocorrelation function is an even function of τ. In addition $\phi_{vv}(0)$ is equal to the mean-square value of the signal as can be seen from equation (32) and

$$\phi_{vv}(0) \geq \phi_{vv}(\tau). \tag{34}$$

As T approaches infinity, the autocorrelation function approaches the square of the mean value of the signal.

The cross-correlation function is analogous to the autocorrelation function. It is applicable to a pair of signals rather than a single signal and is defined as the ensemble average of signal v at time t_1 and signal u at time t_2 or $(t_1+\tau)$.

$$\phi_{vu}(t_1,\tau) = \widetilde{v(t_1)u(t_1+\tau)}. \tag{35}$$

For a stationary stochastic process, the cross-correlation function may be defined in terms of time averages per the ergodic hypothesis. Thus

$$\phi_{vu}(\tau) = \overline{v(t)u(t+\tau)}, \tag{36}$$

$$\phi_{vu}(\tau) = \lim_{T\to\infty} \frac{1}{2T} \int_{-T}^{T} v(t)u(t+\tau)dt. \tag{37}$$

The cross-correlation function for stationary signals is not an even function of τ. It can be shown, however, that

$$\phi_{vu}(\tau) = \phi_{uv}(-\tau). \tag{38}$$

1.7 Power Density Spectra

The response of a linear system to a stochastic input signal is also stochastic. System analysis may be carried out in the time domain using autocorrelation functions or in the frequency domain using mean-square amplitude density distribution or power density spectra as they are called.

The power density spectrum of a function f(t) is simply $1/(2\pi)$ times the Fourier transform of the autocorrelation function of f(t).

Analysis using power density spectra is of primary concern in this thesis due to its growing application to structural load analysis in the field of aircraft and missiles. Stationary stochastic processes only shall be considered.

It is advantageous in understanding the frequency domain analysis to approach it from the time domain. A linear system, as shown in block diagram form in Fig. 6, is subjected to a

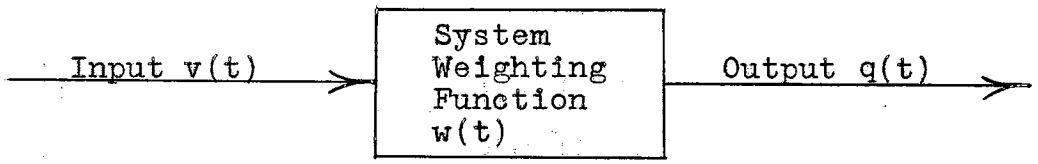

Fig. 6 - Block Diagram of Linear System

stochastic input signal $v(t)$, it has a weighting function $w(t)$, and the stochastic output is $q(t)$.

The autocorrelation function of the output is

$$\phi_{qq}(\tau) = \lim_{T\to\infty} \frac{1}{2T} \int_{-T}^{T} q(t)q(t+\tau)dt; \tag{39}$$

however, from equation (3)

$$q(t) = \int_{-\infty}^{\infty} v(t-t_1)w(t_1)dt_1, \tag{40}$$

and

$$q(t+\tau) = \int_{-\infty}^{\infty} v(t+\tau-t_2)w(t_2)dt_2. \tag{41}$$

Thus equation (39) can be rewritten in terms of the input signal and the system weighting function by substituting equations (40) and (41) in equation (39).

$$\phi_{qq}(\tau) = \lim_{T\to\infty} \frac{1}{2T} \int_{-T}^{T} dt \int_{-\infty}^{\infty} v(t-t_1)w(t_1)dt_1 \int_{-\infty}^{\infty} v(t+\tau-t_2)w(t_2)dt_2. \tag{42}$$

By changing the order of integration and rewriting,

$$\phi_{qq}(\tau) = \int_{-\infty}^{\infty} w(t_1)dt_1 \int_{-\infty}^{\infty} w(t_2)dt_2 \lim_{T\to\infty} \frac{1}{2T} \int_{-T}^{T} v(t-t_1)v(t+\tau-t_2)dt. \tag{43}$$

It can be seen that the last integral on the right is the autocorrelation function of the input signal, therefore,

$$\phi_{qq}(\tau) = \int_{-\infty}^{\infty} w(t_1)dt_1 \int_{-\infty}^{\infty} w(t_2)dt_2 \, \phi_{vv}(\tau+t_1-t_2). \tag{44}$$

Now to switch to the frequency domain, take the Fourier transform of both sides of equation (44).

$$\int_{-\infty}^{\infty} e^{-i\omega\tau} \phi_{qq}(\tau)d\tau =$$

$$\int_{-\infty}^{\infty} e^{-i\omega\tau} d\tau \int_{-\infty}^{\infty} w(t_1)dt_1 \int_{-\infty}^{\infty} w(t_2)\phi_{vv}(\tau+t_1-t_2)dt_2. \quad (45)$$

As previously stated, $1/(2\pi)$ times the Fourier transform of the autocorrelation function of a time function is, by definition, the power density spectrum of that time function; thus

$$\Phi_{qq}(i\omega) = \frac{1}{2\pi} \int_{-\infty}^{\infty} e^{-i\omega\tau} \phi_{qq}(\tau)d\tau. \quad (46)$$

By multiplying both sides of equation (45) by $1/(2\pi)$ and changing the order of integration of the right side:

$$\Phi_{qq}(i\omega) = \int_{-\infty}^{\infty} e^{i\omega t_1} w(t_1)dt_1 \int_{-\infty}^{\infty} e^{-i\omega t_2} w(t_2)dt_2$$
$$\frac{1}{2\pi} \int_{-\infty}^{\infty} e^{-i\omega(\tau+t_1-t_2)} \phi_{vv}(\tau+t_1-t_2)d\tau. \quad (47)$$

Recognizing the Fourier transforms on the right, equation (48) may be written:

$$\Phi_{qq}(i\omega) = W(-i\omega)W(i\omega)\, \Phi_{vv}(i\omega). \quad (48)$$

Simplification may be achieved by recalling Euler's relation

$$e^{i\omega t} = \cos \omega t + i \sin \omega t,$$
$$e^{-i\omega t} = \cos \omega t - i \sin \omega t. \quad (49)$$

The equations for $W(i\omega)$ and $W(-i\omega)$ are then

$$W(i\omega) = \int_{-\infty}^{\infty} e^{-i\omega t} w(t)dt, \quad (50)$$

$$W(i\omega) = \int_{-\infty}^{\infty} w(t)\cos \omega t\, dt - i \int_{-\infty}^{\infty} w(t)\sin \omega t\, dt, \quad (51)$$

and

$$W(-i\omega) = \int_{-\infty}^{\infty} e^{i\omega t} w(t)dt, \quad (52)$$

$$W(-i\omega) = \int_{-\infty}^{\infty} w(t)\cos \omega t\, dt + i \int_{-\infty}^{\infty} w(t)\sin \omega t\, dt, \quad (53)$$

and it is seen that $W(-i\omega)$ and $W(i\omega)$ are conjugate pairs. Therefore,

$$W(-i\omega)W(i\omega) = \left|W(i\omega)\right|^2, \tag{54}$$

and

$$\Phi_{qq}(i\omega) = \left|W(i\omega)\right|^2\Phi_{vv}(i\omega). \tag{55}$$

Equation (55) is the key equation to the analysis of linear system response to a stochastic input.

Frequently, the parameter sought in the system analysis is the mean-square value of the response. This can be obtained by inverse transformation of the output power density spectrum which yields the autocorrelation function; evaluation at $\tau = 0$ gives the mean-square value.

$$\phi_{qq}(\tau) = \int_{-\infty}^{\infty} e^{i\omega\tau}\Phi_{qq}(i\omega)d\omega. \tag{56}$$

$\phi_{qq}(0)$ = mean-square value of f(t) as indicated by equation (32).

$$\phi_{qq}(0) = \int_{-\infty}^{\infty} \Phi_{qq}(i\omega)d\omega. \tag{57}$$

Thus the mean-square value of the stochastic response is equal to the area under the power density spectrum curve for the output. This fact is particularly useful in dealing with stationary stochastic signals having a Gaussian distribution. In this case the probability-density distribution of the response is defined by equation (58).

$$p(q) = \frac{1}{\sigma\sqrt{2\pi}} e^{\frac{-(q-\bar{q})^2}{2\sigma^2}}, \tag{58}$$

where

σ = root-mean-square value of the response, which is $[\phi_{qq}(0)]^{1/2}$ and is termed the standard deviation,

q = system output or response,

$\bar{q} = \lim_{T \to \infty} \frac{1}{2T} \int_{-T}^{T} q(t)dt$.

CHAPTER II

METHODS FOR THE EVALUATION OF AIRCRAFT GUST LOADS USING POWER DENSITY SPECTRA

2.1 Historical Resume

The analytical determination of aircraft structural loads produced by wind gusts has been accomplished for years assuming discrete gusts of specified magnitudes and a (1 - cosine) or other arbitrary shape.(4) These procedures have been adequate but not wholly satisfactory particularly for the definition of fatigue load histories due to gusts.

Approximately ten years ago Clementson (5) investigated the use of power density spectra for definition of the atmospheric turbulence. From this start the application of generalized harmonic analysis methods to the determination of gust loads on aircraft has been investigated and developed extensively by Press (6-8), Mazelsky (6), Meadows and Hadlock (7), and Steiner (8) with the National Aeronautics and Space Administration[1] as well as others.

During 1960, new military specifications for Airplane Strength and Rigidity were adopted. One of these, MIL-A-8866 (ASG) "Reliability Requirements, Repeated Loads, and Fatigue,"

---

[1]Formerly the National Advisory Committee for Aeronautics.

requires the use of power density spectra methods for the determination of aircraft fatigue loads due to atmospheric turbulence. Thus the method has reached a stature of unavoidable importance to the aircraft designer.

2.2 Power Spectra of Atmospheric Turbulence

The power density spectra of atmospheric turbulence have been measured in airplane flights and also from meteorological towers. Measured data from references (6), (7), and (9) are presented in Fig. 7. The frequency argument of these power density spectra plots has been changed from ω to the reduced frequency Ω, which is ω/V, in order to make them independent of the aircraft velocity at the time of measurement. In addition, the magnitude of the power density spectrum function[2], $\Phi(\Omega)$, is two times that which would be expected by the definition of equation (46) since the negative frequency and positive frequency components have been added together and plotted against positive values only of Ω.

The power density spectra of Fig. 7 have generally the same shape but different areas under the curves. This indicates that the power density spectra represent different mean-square intensities of gust velocity but the same relative distribution of amplitude with respect to the reduced frequency.

---

[2]The formally correct nomenclature, $\Phi(i\Omega)$, is discarded in favor of $\Phi(\Omega)$ since this is more commonly used in aeronautical references.

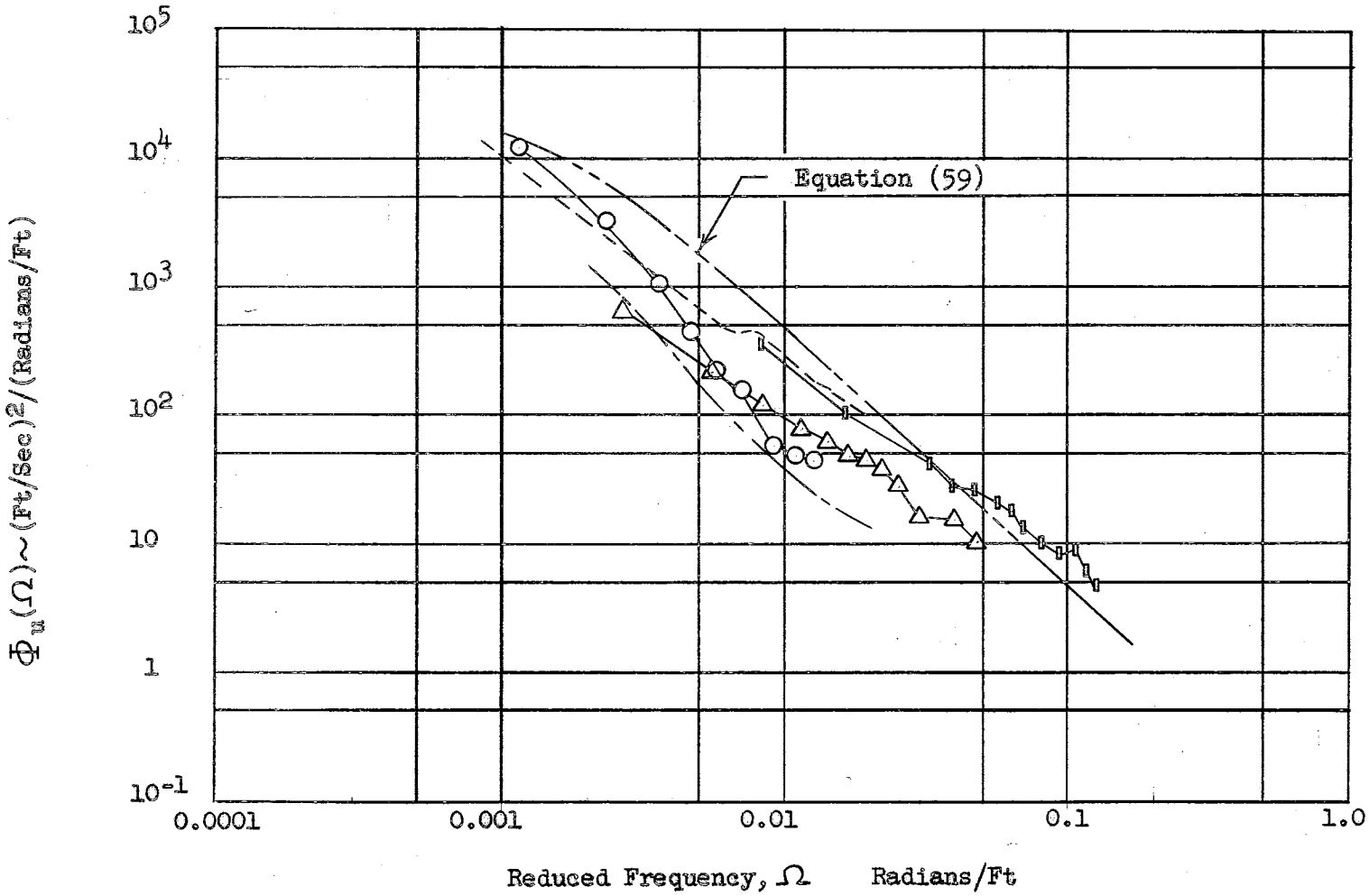

Fig. 7 Power Density Spectra of Atmospheric Turbulence

A general equation for the power density spectra of atmospheric turbulence is stated by Press, Meadows, and Hadlock (7).

$$\Phi_u(\Omega) = \sigma_u^2 \frac{L}{\pi} \frac{1+3\Omega^2L^2}{(1+\Omega^2L^2)^2}, \qquad (59)$$

where

$\Phi_u(\Omega)$ = power density spectrum of gust velocity in $(\text{ft./sec.})^2/(\text{radians/foot})$.

Ω = reduced frequency ω/V in radians/foot.

L = scale of turbulence in feet.

σ_u^2 = mean-square gust velocity in $(\text{feet/second})^2$.

L can be considered to be proportional to the average eddy size of the turbulence. A value of L of 1,000 feet has been used in reference (7), (8), and (9), to give the best fit to measured data. A plot of equation (59) using $\sigma_u^2 = 49$ $(\text{ft./sec.})^2$ is shown in Fig. 7 for comparison with the experimental data.

2.3 Gaussian Distribution of Atmospheric Turbulence

In general, an airplane may be considered a linear system in the determination of its response to a gust input. As stated by Truxal(3), page 418, "..... a signal which possesses a Gaussian distribution function still has this type of distribution after passing through any linear network." Thus flight measurements of an airplane response parameter such as the normal acceleration, a_n, at the center of gravity have been investigated to determine their probability distribution in order to establish the probability

distribution of the input gust velocities.

Press and Mazelsky (6) theorize that local atmospheric turbulence may be considered a stationary stochastic process with gust velocities distributed in a normal or Gaussian manner. This trend is indicated, for example, by flight test data presented by Press and Mazelsky (6) representing center of gravity acceleration peaks measured during a two minute interval for each of two similar airplanes in side by side flight at 450 miles per hour.

Overall atmospheric turbulence, as opposed to local atmospheric turbulence, is not distributed in a Gaussian manner due to variations with weather, terrain and altitude. Press, Meadows, and Hadlock (7) have investigated data on peak values of airplane center of gravity normal accelerations measured during approximately 7,000 flight hours accrued in eight different transport operations. The investigation shows that, although the data for each operation do not conform to a Gaussian distribution, they could represent the summation of several different Gaussian distributions. These investigators have concluded that overall atmospheric turbulence is made up of elemental stationary stochastic processes having individual Gaussian distributions.

The majority of airplane gust load data which have been accumulated for statistical evaluation are in the form of acceleration peak counts recorded at very low film speeds (2 to 8 feet/hour) and are not suited for determination of correlation functions. Press, Meadows, and Hadlock (7) have developed a method to convert these data to a form applicable

to power density spectra analysis. The conversion is based on equation (60), developed by Rice (10) which applies to a Gaussian distribution of a_n.

$$N(a_n) = \frac{1}{2\pi}\left[\frac{\int_o^\infty \omega^2 \Phi_{a_n}(\omega)d\omega}{\int_o^\infty \Phi_{a_n}(\omega)d\omega}\right]^{1/2} e^{\frac{-a_n^2}{2\sigma_{a_n}^2}}, \qquad (60)$$

where

$N(a_n) \approx$ average number of maximum accelerations per second exceeding a_n,

$\Phi_{a_n}(\omega)$ = power density spectrum of $a_n(t)$,

$\sigma_{a_n}^2 = \int_o^\infty \Phi_{a_n}(\omega)d\omega$.

This equation is the exact expression for the number of crossings per second with positive slope of given values of a_n. It is an approximate expression for the number of positive acceleration peaks per second above a given value of a_n; it becomes increasingly exact as a_n increases.

Making use of equation (59) as defining the power density spectrum of atmospheric turbulence and recalling equation (55) it can be seen that the portion of equation (60) within the brackets is a constant for a given airplane under given operating conditions of speed, weight, altitude, etc.; $1/(2\pi)$ times this constant is termed N_o.

$$N_o = \frac{1}{2\pi}\left[\frac{\int_o^\infty \omega^2 \Phi_{a_n}(\omega)d\omega}{\int_o^\infty \Phi_{a_n}(\omega)d\omega}\right]^{1/2}. \qquad (61)$$

N_o is the exact expression for the number of times per second that $a_n(t)$ crosses the value zero with positive slope. Rewriting equation (60),

$$N(a_n) = N_o e^{\frac{-a_n^2}{2\sigma_{a_n}^2}}, \tag{62}$$

$$\log N(a_n) = \log N_o - \frac{1}{2\sigma_{a_n}^2} a_n^2. \tag{63}$$

The linear relationship of equation (63), which is applicable to a Gaussian distribution of a_n, has been used in conjunction with the peak acceleration data from each of the eight different transport operations to reach the conclusion that although these data for any one operation do not fit the linear relationship and, therefore, do not conform to a single Gaussian distribution, they could represent the sum of several Gaussian distributions each having a different σ.(7) The feasibility of this is shown in Fig. 8 which is a plot of the peak acceleration data from one of the eight transport operations.

$\overline{M(a_n)}$ is the average number of positive acceleration peaks per second exceeding given values of a_n. The ordinate of Fig. 8 is $2\ \overline{M(a_n)}$ because the transport operation acceleration peak count data included both positive and negative peak counts. Linear relationships representing three separate Gaussian distributions are also plotted; the sum of these is the short dashed curve which closely approximates the measured data. In equation form,

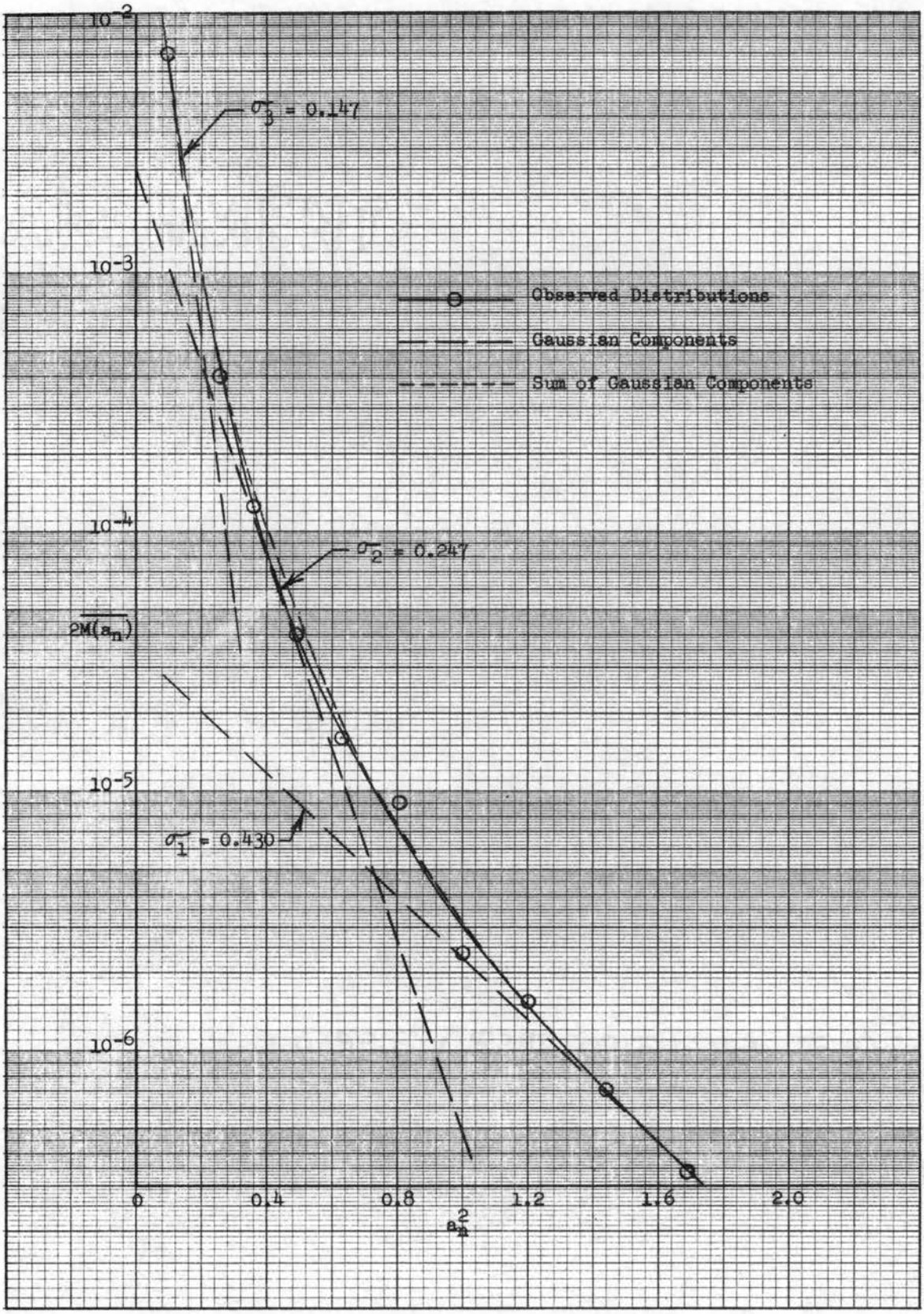

Fig. 8 Peak Acceleration Data From A Transport Operation

$$\overline{M(a_n)} = \sum_{i=1}^{k} P_i \, N_i(a_n), \tag{64}$$

$$\overline{M(a_n)} = \sum_{i=1}^{k} (N_o)_i \, P_i \, e^{\frac{-a_n^2}{2\sigma_i^2}}. \tag{65}$$

where P_i is the proportion of total flight at the i^{th} condition and $N_i(a_n)$ is the number of peak accelerations per second exceeding given values of acceleration for the i^{th} condition. If we consider average values of airplane weight, speed, altitude, etc. which go into the calculation of $|W(i\Omega)|^2$ used to calculate $\Phi_{a_n}(\Omega)$ from $\Phi_u(\Omega)$ by equation (55) and therefore define an average N_o, equation (65) may be written as

$$\overline{M(a_n)} = N_o \sum_{i=1}^{k} P_i \, e^{\frac{-a_n^2}{2\sigma_i^2}}. \tag{66}$$

An airplane in long time flight will encounter conditions of air turbulence which are continually varying in intensity as defined by the root mean-square gust velocity in equation (59). Considering this fact, equation (66) is rewritten in the following form:

$$M(a_n) = N_o \int_o^\infty f(\sigma_{a_n}) e^{\frac{-a_n^2}{2\sigma_{a_n}^2}} d\sigma_{a_n}, \tag{67}$$

where $f(\sigma_{a_n}) \, d\sigma_{a_n}$ gives the proportion of flight time spent at values of σ_{a_n} between σ_{a_n} and $\sigma_{a_n} + d\sigma_{a_n}$. Thus $f(\sigma_{a_n})$ is the probability-density distribution of the root mean-square acceleration.

The transport operation data are analyzed in Reference (7) to determine the applicable probability-density distribution of σ_{a_n}. Three equations are developed therein as possibilities:

$$\left.\begin{aligned} f_1(\sigma_{a_n}) &= \frac{1}{a_1}\sqrt{\frac{2}{\pi}}\, e^{\frac{-\sigma_{a_n}^2}{2a_1^2}}, \\ f_2(\sigma_{a_n}) &= \frac{1}{a_2}\, e^{\frac{-\sigma_{a_n}}{a_2}}, \\ f_3(\sigma_{a_n}) &= \frac{1}{2a_3^2}\, e^{\frac{-\sqrt{\sigma_{a_n}}}{a_3}}. \end{aligned}\right\} \quad (68)$$

In each equation, a is a scale parameter with high values of a associated with more severe turbulence. The equation for $f_1(\sigma_{a_n})$ has been proposed by Press and Steiner in the later work of Reference (6) for prediction of gust loads.

From equation (57)

$$\sigma_{a_n}^2 = \int_0^\infty \Phi_{a_n}(\omega)\, d\omega. \quad (69)$$

Substituting the assumed equation for the power density spectra of atmospheric turbulence, (59), into equation (69), along with the relation of equation (55), the relation between σ_{a_n} and σ_u is established:

$$\left(\frac{\sigma_{a_n}}{\sigma_u}\right)^2 = \frac{L}{\pi}\int_0^\infty \frac{1+3\Omega^2L^2}{(1+\Omega^2L^2)^2}\left|W(i\Omega)\right|^2 d\Omega, \quad (70)$$

where

$W(i\Omega)$ = the system transfer function in terms of the reduced frequency Ω which is ω/V.

This may be written as

$$\sigma_{a_n} = \bar{A}\sigma_u, \tag{71}$$

where

$$\bar{A} = \left[\frac{L}{\pi}\int_0^\infty \frac{1+3\Omega^2L^2}{(1+\Omega^2L^2)^2}\left|W(i\Omega)\right|^2 d\Omega\right]^{1/2}. \tag{72}$$

$\bar{A}$ is a constant for a specific $\left|W(i\Omega)\right|^2$.

Making use of equation (71) to change the variable of equation (68) for $f_1(\sigma_{a_n})$, the following equation develops for the probability-density distribution of the root mean-square gust velocity:

$$\hat{f}(\sigma_u) = \bar{A}\, f(\sigma_{a_n}),$$

$$\hat{f}(\sigma_u) = \frac{1}{b}\sqrt{\frac{2}{\pi}}\, e^{\frac{-\sigma_u^2}{2b^2}}, \tag{73}$$

where $b = a/\bar{A}$.

Appropriate values of the scale parameter, b, have been developed by Press and Steiner (8) to define $\hat{f}(\sigma_u)$ for altitudes from sea level to 60,000 feet and for both non-storm and storm turbulence. These are set forth in Section 2.4.

It is appropriate to replace σ_{a_n} in equation (67) with σ_u which is the actual basic input parameter for gust load studies. Knowing that $f(\sigma_{a_n}) = (1/\bar{A})\,\hat{f}(\sigma_u)$, then

$$\overline{M(a_n)} = N_o \int_o^\infty \hat{f}(\sigma_u) e^{\frac{-a_n^2}{2\bar{A}^2\sigma_u^2}} d\sigma_u. \qquad (74)$$

In this equation both N_o and $\bar{A}$ are functions of the power density spectrum for atmospheric turbulence for σ_u = 1.0 ft/sec. and the system transfer function. As previously stated, each are constants for a given airplane under a given set of average operating conditions of weight, velocity, altitude, etc. Equation (74) is then a key equation for evaluating statistically the airplane loads due to gusts.

2.4 Gust Encounter History to be Considered in Airplane Design

The anticipated atmospheric turbulence to be encountered in operational flight has been investigated by Press and Steiner (8). Two types of turbulence have been considered, moderately rough clear air turbulence termed nonstorm turbulence and severe turbulence encountered in thunderstorms, termed storm turbulence. Proportions of the total flight distance during which each type of turbulence may be anticipated have also been estimated. The probability-density distribution for the root mean-square gust velocity, equation (73), may be modified as follows to account for each of these types of turbulence:

$$\hat{f}(\sigma_u) = P_1 \frac{1}{b_1}\sqrt{\frac{2}{\pi}} e^{\frac{-\sigma_u^2}{2b_1^2}} + P_2 \frac{1}{b_2}\sqrt{\frac{2}{\pi}} e^{\frac{-\sigma_u^2}{2b_2^2}}, \qquad (75)$$

where

P_1 = proportion of total flight distance in nonstorm turbulence.

P_2 = proportion of total flight distance in storm turbulence.

b_1 = nonstorm turbulence scale factor.

b_2 = storm turbulence scale factor.

Table I has been taken from Military Specification MIL-A-8866(ASG). It defines the parameters of equation (75) which must be used in gust load evaluations for military airplanes. Basically it was developed by Press and Steiner(8) but has been modified to require consideration of a larger proportion of flight distance in storm turbulence.

TABLE I

TURBULENCE PARAMETERS

Altitude Ft. x 10^{-3}	P_1	P_2	b_1	b_2	L Feet
0 - 1	1.0	0	3.9	-	500
1 - 2	0.32	0.0004	4.6	9.4	1,000
2 - 10	0.08	0.00125	3.8	9.8	1,000
10 - 20	0.045	0.0015	3.7	10.4	1,000
20 - 30	0.06	0.0012	3.5	11.2	1,000
30 - 40	0.065	0.0006	3.4	11.1	1,000
40 - 50	0.023	0.0002	3.1	11.7	1,000
50 - 60	0.02	0.0001	2.8	12.5	1,000

Press and Steiner (8) consider a slightly modified version of equation (74).

$$\bar{G}(y) = G_o \int_o^\infty \hat{f}(\sigma_u) e^{\frac{-y^2}{2\sigma_u^2 \bar{A}^2}} d\sigma_u, \tag{76}$$

where

$\bar{G}(y) \approx$ average number of response peaks exceeding given values of y (total of both positive and negative peaks) per mile of flight.

y = any desired response parameter for the airplane system. It could be a_n but could just as well be wing bending moment, etc.

$G_o \approx$ average number of response peaks per mile of flight in rough air.

In this equation

$$G_o = \frac{(2)\ (1.467)\ (3600)}{V} N_o. \tag{77}$$

N_o is defined by equation (61) for the specific response parameter required and V is the airplane speed in ft/sec. It is important to note that the factor (2) is necessary since $\bar{G}(y)$ defines the sum of positive and negative response peaks whereas $\overline{M(a_n)}$ defines the positive response peaks only.

Substitution of equation (75) into equation (76) and integrating yields

$$\bar{G}(y) = P_1 G_o e^{-y/(b_1 \bar{A})} + P_2 G_o e^{-y/(b_2 \bar{A})}, \tag{78}$$

which is a relatively simple equation, and can be used directly to define the anticipated gust load history for an airplane. (8)

Suppose, for example, a given airplane is to frequently fly the mission indicated by Fig. 9 and the gust load spectrum for this mission is required.

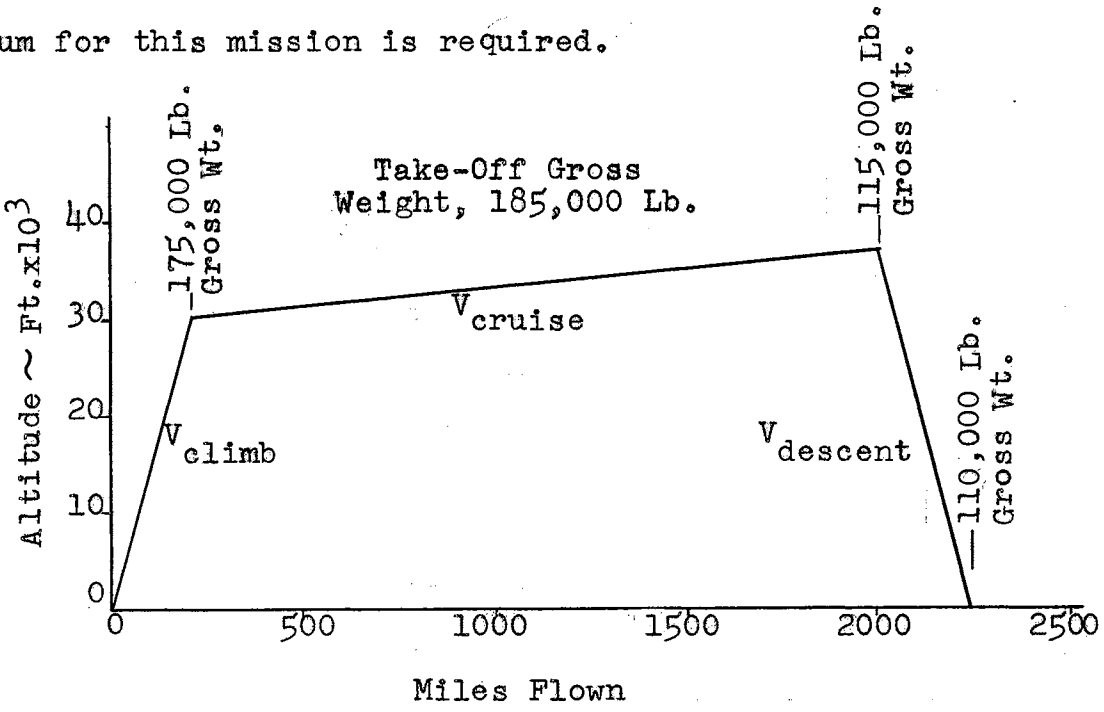

Fig. 9 - Typical Mission Flight Profile

The mission must be broken down into segments for which average values of b_1, b_2, P_1, P_2, $\bar{A}$, and G_o can be determined. For, say the i^{th} segment, these applicable average parameters are used to calculate $\bar{G}_i(y)$. The product of $\bar{G}_i(y)$ and the number of miles flown in the i^{th} segment, D_i, gives the number of response peaks exceeding given value of y which are encountered in that i^{th} segment only. By repetition of this procedure for all segments of the mission and summation of the results, the gust load history for the entire mission is determined. This can be stated in equation form as

$$\bar{G}_t(y) = \sum_{i=1}^{n} D_i \bar{G}_i(y), \tag{79}$$

where

$\overline{G}_t(y)$ = expected number of response peaks exceeding given values of y.

D_i = flight distance in i^{th} flight segment.

$\overline{G}_i(y)$ = response history in the i^{th} segment from equation (78).

The total gust load history for the life of the airplane can be estimated by defining the various missions anticipated for normal operational use of the airplane, the number of times each should be flown per year, and the desired number of years the airplane is to remain operational. Application of equation (79) to this total operational plan will provide the desired fatigue gust loading information for design and testing.

2.5 Current Gust Study Efforts

An extensive flight survey of atmospheric turbulence at altitudes below 2,000 feet has recently been completed by the Douglas Aircraft Company, Inc. under an Air Force contract. The final report of this study is to be published in the near future. Reference (9) is an interim report on subject.

A similar high altitude study of atmospheric turbulence is to be carried out, on a similar contract arrangement, in the near future.

These efforts and other similar ones of recent origin are basically for the purpose of better defining atmospheric turbulence in power density spectrum terms. The data gathering and reduction procedures used are optimized for the purpose, making use of high speed computing machines to reduce vast amounts of flight data.

CHAPTER III

INVESTIGATION OF THE EFFECT OF PYLON STRUCTURAL FLEXIBILITY ON GUST INERTIA LOADS EXPERIENCED BY THE SUPPORTED STORES

3.1 Objective of Investigation

Airplanes present many examples of large high density items which are mounted to the basic airframe by flexible support structure. Among these are jet engines, equipment pods, bombs, missiles, fuel tanks, and the other stores which are pylon or strut mounted to the wing or fuselage.

In general, each pylon structure is designed to assure capability to carry its supported item or items throughout the complete velocity envelope of maneuver and gust load factors for the associated airplane. The resulting inertia and air loads are treated as steady state loads in the stress analysis of the structure. In addition, certain basic minimum stiffness requirements may be assigned to the pylon structure to assure freedom from flutter.

The fatigue strength of the pylon is investigated analytically and in the laboratory on the basis of the cyclic load history data developed for the associated airplane, to assure adequate structural life.

In the development of the cyclic fatigue load history for the pylon and supported store, it has been common engi-

neering practice to ignore the effect that pylon structural flexibility may have in altering the accelerations felt by the supported store as compared to those input at the point where the pylon attaches to the basic airframe.

The significance of considering the effect of pylon flexibility is investigated herein for a hypothetical example. This effort is pursued in the belief that a supported store may feel not only an amplification or attenuation of the basic input accelerations but also induced accelerations acting in directions which differ from the basic input. Further it is felt that these induced accelerations may, in some cases, have primary significance in a structural fatigue investigation.

An inverted Y shaped pylon is considered as shown in Fig. 10. This pylon is attached to comparatively rigid basic wing structure and supports two high mass stores, one from each arm of the inverted Y.

A power density spectrum of vertical or normal incremental acceleration input at the pylon to wing attachment point, due to atmospheric gusts, is given in Fig. 11. This is applicable to high speed low level flight, at a specific gross weight, in homogeneous atmospheric turbulence having a root mean-square intensity, σ_u, of 20 ft/sec.

The deflection influence coefficients for the pylon structure are given in Table II. These coefficients define the deflections of the center of gravity of each store due to unit loads applied separately at the center of gravity of each store. In reality, each store has six degrees of free-

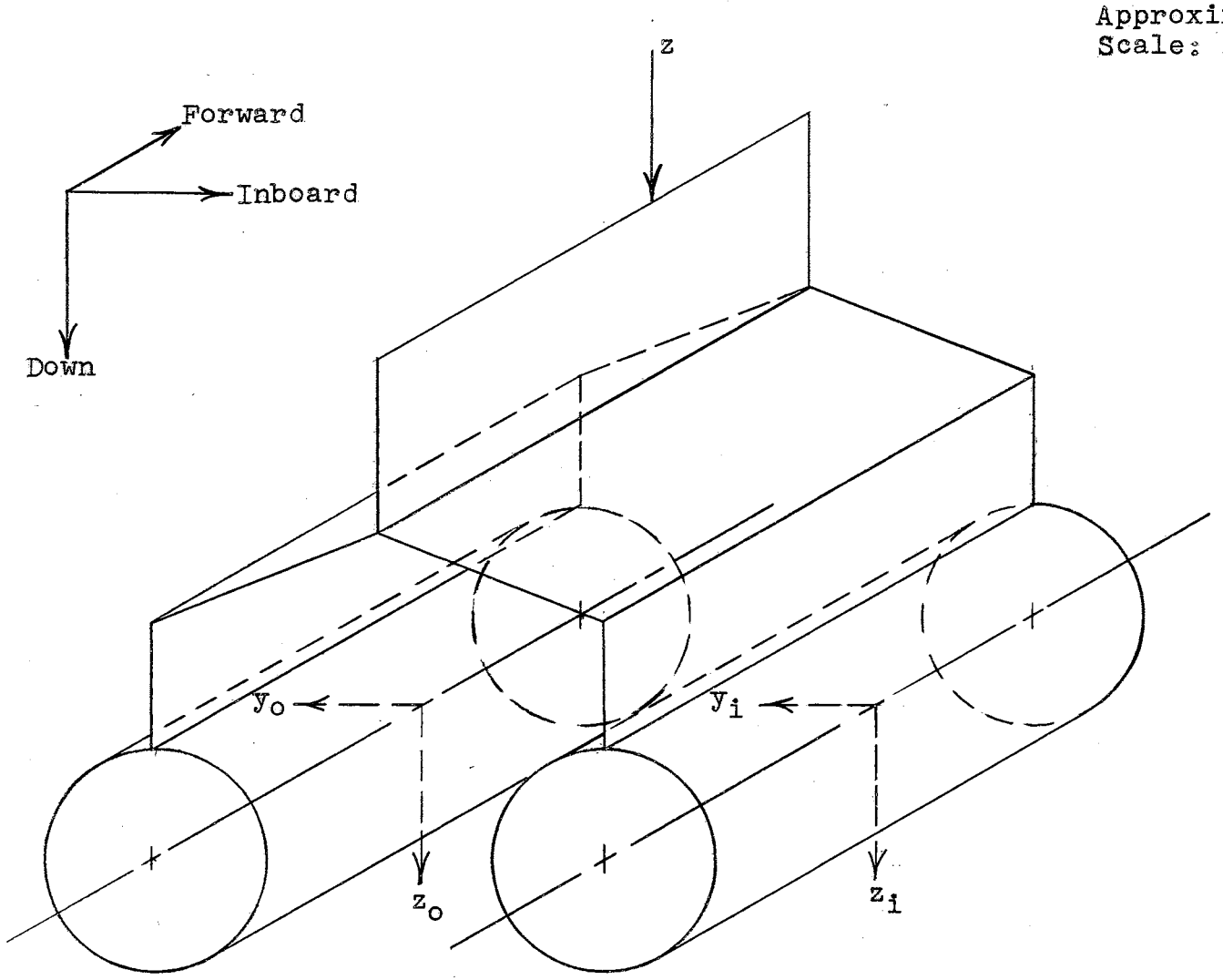

Fig. 10 - Pylon Line Diagram

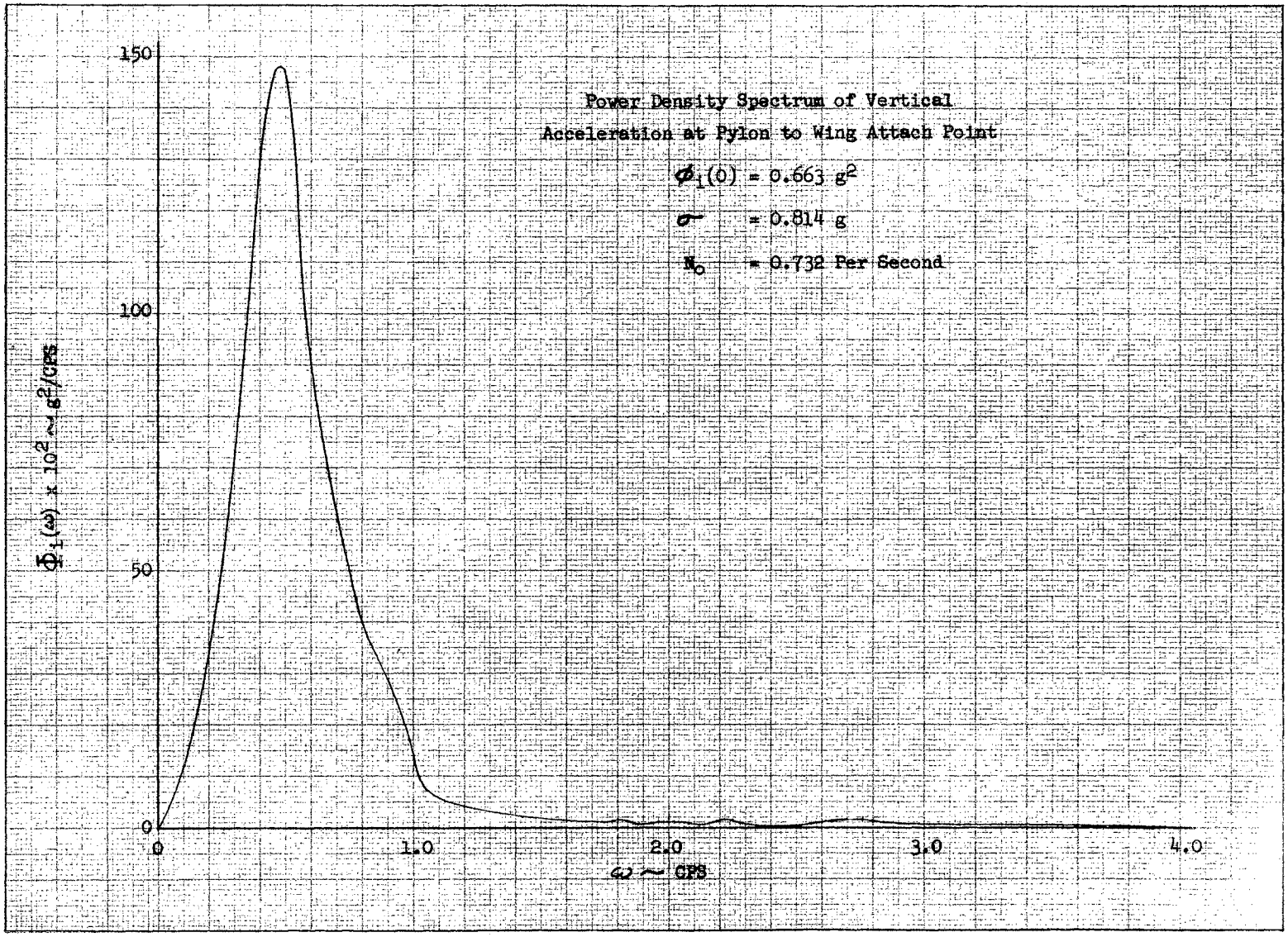

Fig. 11 Input Power Density Spectrum

TABLE II

PYLON DEFLECTION INFLUENCE COEFFICIENTS

Location and Direction of Applied Unit Load / Resulting Deflections		Center of Gravity of Outb'd. Store		Center of Gravity of Inb'd. Store	
		Vertical	Lateral	Vertical	Lateral
Center of Gravity of Outboard Store	Vertical	29.15936	-34.75498	-13.19916	-21.70206
	Lateral	-34.75498	78.56017	24.75696	37.88529
Center of Gravity of Inboard Store	Vertical	-13.19916	24.75696	25.35924	38.09839
	Lateral	-21.70206	37.88529	38.09839	92.52996

Notes:

1. Units are inches x 10^{-6} per pound.
2. Origin of each coordinate system is at C.G. of that specific store.
3. Positive vertical deflection or load is down.
4. Positive lateral deflection or load is outboard.
5. This array of coefficients (times 10^{6} to put in units of inches per pound) is used herein as Matrix G where the first row is G_{11}, G_{12}, G_{13}, G_{14}; the second row G_{21}, G_{22}, G_{23}, G_{24}; etc.

dom. All could be considered in a complete investigation of this type, using high speed digital computing machines; however, simplifying assumptions have been made herein to keep the calculations within bounds for a desk calculator. The store itself has been assumed infinitely rigid and the pylon has been assumed flexible in the vertical and lateral directions only with infinite stiffness for longitudinal loads and all moments applied at the store centers of gravity. Although these assumptions have been made to simplify the problem, they are reasonable for the type of structure considered. The influence coefficients are derived as a normal part of the pylon static stress analysis and the values of Table II are entirely realistic for such a store supporting pylon designed to meet military structural design criteria. An assumed mass of thirty five pound seconds squared/inch has been chosen.

A review of the deflection influence coefficients of Table II indicates that large lateral deflections result from the application of a vertical load at a store center of gravity. The lateral deflection is altered by simultaneous application of an equal vertical load at the center of gravity of the opposite store. In each case, however, the lateral deflection, due to vertical load application, is quite significant. This would indicate that the vertical gust load factor or acceleration input at the pylon to wing attach point may induce significant lateral acceleration at the center of gravity of each store. In order to evaluate the results of this investigation, it will be considered that the basic structure is statically designed such that a lateral load

factor or acceleration of 1.0 "g" at the center of gravity of the store produces a critical stress which is equivalent to that produced by a vertical load factor at the center of gravity of the store of 2.75 "g." This relationship will be used as a means of conveniently combining the effects of the total cyclic load history developed in this investigation.

3.2 Development of System Transfer Functions

Referring to Fig. 10, pylon elastic deflection equations (80) are written in matrix form. Matrix G is the matrix of pylon deflection influence coefficients from Table II. The subscript i applies to the inboard store and subscript o applies to the outboard store. The input to the system is vertical displacement z which is input at the pylon to wing attachment point as a unit impulse function. Each value of F is the pylon spring force related to the net pylon deflections in the y and z directions.

$$\begin{Bmatrix} z_o - z \\ y_o \\ z_i - z \\ y_i \end{Bmatrix} = \begin{bmatrix} G_{11} & G_{12} & G_{13} & G_{14} \\ G_{21} & G_{22} & G_{23} & G_{24} \\ G_{31} & G_{32} & G_{33} & G_{34} \\ G_{41} & G_{42} & G_{43} & G_{44} \end{bmatrix} \begin{Bmatrix} F_{z_o} \\ F_{y_o} \\ F_{z_i} \\ F_{y_i} \end{Bmatrix} \quad (80)$$

Then the pylon spring force equations are

$$\begin{Bmatrix} F_{z_o} \\ F_{y_o} \\ F_{z_i} \\ F_{y_i} \end{Bmatrix} = \begin{bmatrix} K_{11} & K_{12} & K_{13} & K_{14} \\ K_{21} & K_{22} & K_{23} & K_{24} \\ K_{31} & K_{32} & K_{33} & K_{34} \\ K_{41} & K_{42} & K_{43} & K_{44} \end{bmatrix} \begin{Bmatrix} z_o - z \\ y_o \\ z_i - z \\ y_i \end{Bmatrix} \quad (81)$$

where the [K] matrix is the inverse of [G] and is shown in Table III.

TABLE III

MATRIX OF SPRING CONSTANTS, [K]

$$\begin{bmatrix} 0.07449201 & 0.02990851 & 0.004451749 & 0.00336569 \\ 0.02990851 & 0.03039817 & -0.01559786 & 0.000990886 \\ 0.00451749 & -0.01559786 & 0.12014453 & -0.04202255 \\ 0.00336569 & 0.000990886 & -0.04202255 & 0.0284934 0 \end{bmatrix} \times 10^6$$

NOTE: Units are pounds per inch

In a power spectral density analysis we are, by definition, dealing with a harmonic representation of the disturbing function. It is therefore appropriate to consider the structural damping in the system in the manner commonly employed in structural vibration analyses of harmonically oscillating systems. This is a damping proportional to displacement but in phase with the velocity.(12) The equation of motion for the system will have the form

$$M\ddot{x} + cK|x|\frac{\dot{x}}{|\dot{x}|} + Kx = 0 , \quad (82)$$

where

c = structural damping coefficient.

K = spring constant.

Since the system response is harmonic, $x = x_o e^{i\omega t}$. Substituting this in equation (82),

$$M\ddot{x} + (1 + ic) Kx = 0. \tag{83}$$

In the form of equation (83) then, the differential equations for the pylon/store system are

$$\left.\begin{aligned} M_o \ddot{z}_o + (1 + ic) F_{z_o} &= 0 \\ M_o \ddot{y}_o + (1 + ic) F_{y_o} &= 0 \\ M_i \ddot{z}_i + (1 + ic) F_{z_o} &= 0 \\ M_i \ddot{y}_i + (1 + ic) F_{y_i} &= 0 \end{aligned}\right\} \tag{84}$$

The values of the F terms are defined by equations (81). The icF terms represent structural damping which opposes the motion; as previously stated, the magnitude of the damping force is assumed proportional to the elastic restoring force but in phase with the velocity. A value of .03 has been chosen for c in this investigation. For metal aircraft structures, this value is consistent with the typical values given by Scanlon and Rosenbaum (12) page 87 and somewhat high compared to the measured values quoted by Fung (13) on page 227. No other damping is considered.

These equations may be simplified by dividing each side by M_o or M_i which are assumed equal and by (1 + ic) to obtain

equations (85)

$$\left.\begin{aligned}
&\ddot{z}_o \left(\frac{1}{1+ic}\right) + \frac{1}{M} F_{z_o} = 0 \\
&\ddot{y}_o \left(\frac{1}{1+ic}\right) + \frac{1}{M} F_{y_o} = 0 \\
&\ddot{z}_i \left(\frac{1}{1+ic}\right) + \frac{1}{M} F_{z_i} = 0 \\
&\ddot{y}_i \left(\frac{1}{1+ic}\right) + \frac{1}{M} F_{y_i} = 0
\end{aligned}\right\} \quad (85)$$

The Fourier transformation of equations (85), considering the input z to be a unit impulse, yields the following set of simultaneous equations in the frequency domain where K_{11}, K_{12}, etc. refer to the corresponding elements of the spring constant matrix [K] defined in Table III:

$$\left.\begin{aligned}
&Z_o(i\omega)\left[\frac{-\omega^2}{1+ic}+\frac{K_{11}}{M}\right]+\frac{K_{12}}{M}Y_o(i\omega)+\frac{K_{13}}{M}Z_i(i\omega)+\frac{K_{14}}{M}Y_i(i\omega) = \frac{K_{11}+K_{13}}{M} \\
&\frac{K_{21}}{M}Z_o(i\omega)+Y_o(i\omega)\left[\frac{-\omega^2}{1+ic}+\frac{K_{22}}{M}\right]+\frac{K_{23}}{M}Z_i(i\omega)+\frac{K_{24}}{M}Y_i(i\omega) = \frac{K_{21}+K_{23}}{M} \\
&\frac{K_{31}}{M}Z_o(i\omega)+\frac{K_{32}}{M}Y_o(i\omega)+Z_i(i\omega)\left[\frac{-\omega^2}{1+ic}+\frac{K_{33}}{M}\right]+\frac{K_{34}}{M}Y_i(i\omega) = \frac{K_{31}+K_{33}}{M} \\
&\frac{K_{41}}{M}Z_o(i\omega)+\frac{K_{42}}{M}Y_o(i\omega)+\frac{K_{43}}{M}Z_i(i\omega)+Y_i(i\omega)\left[\frac{-\omega^2}{1+ic}+\frac{K_{44}}{M}\right] = \frac{K_{41}+K_{43}}{M}
\end{aligned}\right\} \quad (86)$$

or in matrix form

$$\begin{Bmatrix} \frac{K_{11}+K_{13}}{M} \\ \frac{K_{21}+K_{23}}{M} \\ \frac{K_{31}+K_{33}}{M} \\ \frac{K_{41}+K_{43}}{M} \end{Bmatrix} = \begin{bmatrix} \left[\frac{K_{11}}{M} - \frac{\omega^2}{1+ic}\right] & \frac{K_{12}}{M} & \frac{K_{13}}{M} & \frac{K_{14}}{M} \\ \frac{K_{21}}{M} & \left[\frac{K_{22}}{M} - \frac{\omega^2}{1+ic}\right] & \frac{K_{23}}{M} & \frac{K_{24}}{M} \\ \frac{K_{31}}{M} & \frac{K_{32}}{M} & \left[\frac{K_{33}}{M} - \frac{\omega^2}{1+ic}\right] & \frac{K_{34}}{M} \\ \frac{K_{41}}{M} & \frac{K_{42}}{M} & \frac{K_{43}}{M} & \left[\frac{K_{44}}{M} - \frac{\omega^2}{1+ic}\right] \end{bmatrix} \begin{Bmatrix} Z_o(i\omega) \\ Y_o(i\omega) \\ Z_i(i\omega) \\ Y_i(i\omega) \end{Bmatrix} \quad (87)$$

The square matrix on the right of equation (87) is shown in Table IV and is termed matrix [A].

TABLE IV

MATRIX [A]

$$\begin{bmatrix} \left[2128.343 - \frac{\omega^2}{1+ic}\right] & 854.5288 & 129.0711 & 96.16257 \\ 854.5288 & \left[868.5191 - \frac{\omega^2}{1+ic}\right] & -445.6531 & 28.31102 \\ 129.0711 & -445.6531 & \left[3432.700 - \frac{\omega^2}{1+ic}\right] & -1200.644 \\ 96.16257 & 28.31102 & -1200.644 & \left[814.0971 - \frac{\omega^2}{1+ic}\right] \end{bmatrix}$$

then

$$\begin{Bmatrix} Z_o(i\omega) \\ Y_o(i\omega) \\ Z_i(i\omega) \\ Y_i(i\omega) \end{Bmatrix} = \begin{bmatrix} B_{11} & B_{12} & B_{13} & B_{14} \\ B_{21} & B_{22} & B_{23} & B_{24} \\ B_{31} & B_{32} & B_{33} & B_{34} \\ B_{41} & B_{42} & B_{43} & B_{44} \end{bmatrix} \begin{Bmatrix} \frac{K_{11} + K_{13}}{M} \\ \frac{K_{21} + K_{23}}{M} \\ \frac{K_{31} + K_{33}}{M} \\ \frac{K_{41} + K_{43}}{M} \end{Bmatrix} , \quad (88)$$

where the [B] matrix is the inverse of matrix [A].

Equation (88) produces equations (89) through (92) which are the Fourier transforms of the z and y displacements at the center of gravity of each store due to a vertical displacement unit impulse input at the pylon to wing attachment. In general these would be the system transfer functions.

$$Z_o(i\omega) = \frac{-2257.414\lambda^3 + 10,844,478\lambda^2 - 7,484,328,850\lambda + 1,019,981,826,000}{\lambda^4 - 7243.679\lambda^3 + 14,973,060\lambda^2 - 8,054,095,390\lambda + 1,019,983,970,000} ,$$

$$Z_o(i\omega) = \frac{-2257.414(\lambda - 182.916)(\lambda - 616.9123)(\lambda - 4004.1101)}{(\lambda - 184.3014)(\lambda - 547.62833)(\lambda - 2552.501)(\lambda - 3959.248)} . \quad (89)$$

$$Y_o(i\omega) = \frac{-408.8757\lambda^3 + 2,296,196\lambda^2 - 356,928,223\lambda}{\lambda^4 - 7243.679\lambda^3 + 14,973,060\lambda^2 - 8,054,095,390\lambda + 1,019,983,970,000} ,$$

$$Y_o(i\omega) = \frac{-408.8757\lambda(\lambda - 160.0018)(\lambda - 5455.8760)}{(\lambda - 184.3014)(\lambda - 547.6283)(\lambda - 2552.501)(\lambda - 3959.248)} . \quad (90)$$

$$Z_i(i\omega) = \frac{-3561.771\lambda^3 + 12,138,525\lambda^2 - 7,619,989,700\lambda + 1,019,983,850,000}{\lambda^4 - 7243.679\lambda^3 + 14,973,060\lambda^2 - 8,054,095,390\lambda + 1,019,983,970,000} ,$$

$$Z_i(i\omega) = \frac{-3561.771(\lambda - 185.911)(\lambda - 583.8610)(\lambda - 2638.2305)}{(\lambda - 184.3014)(\lambda - 547.6283)(\lambda - 2552.501)(\lambda - 3959.248)} . \quad (91)$$

$$Y_i(i\omega)=\frac{1104.481\lambda^3-3,053,586\lambda^2+585,337,960\lambda}{\lambda^4-7243.679\lambda^3+14,973,060\lambda^2-8,054,095,390\lambda+1,019,983,970,000},$$

$$Y_i(i\omega)=\frac{1104.481\lambda(\lambda-207.2201)(\lambda-2557.5046)}{(\lambda-184.3014)(\lambda-547.6283)(\lambda-2552.501)(\lambda-3959.248)}. \quad (92)$$

where

$$\lambda = \frac{\omega^2}{1+ic}.$$

The introduction of the complex structural damping terms of icF in equations (84), however, produces admittances or transfer functions which are (1+ic) times the steady state transfer functions which are desired. The equations of Table V have been developed by multiplying equations (89) through (92) by $(1+ic)^3/(1+ic)^4$ and represent the steady state transfer functions which are actually sought. These will be designated as $Z_o'(i\omega)$, $Y_o'(i\omega)$, $Z_i'(i\omega)$, and $Y_i'(i\omega)$.

3.3 Power Density Spectra of Response

The power density spectra of the vertical and lateral acceleration at the center of gravity of the outboard store are developed by numerically evaluating $|Z_o'(i\omega)|^2$ and $|Y_o'(i\omega)|^2$ as functions of ω and using equation (55):

$$\Phi_{o_{z_o}}(\omega) = |Z_o'(i\omega)|^2 \Phi_i(\omega), \quad (93)$$

$$\Phi_{o_{y_o}}(\omega) = |Y_o'(i\omega)|^2 \Phi_i(\omega), \quad (94)$$

where $\Phi_i(\omega)$ is defined by Fig. 11. Table VI shows the calculation of $\Phi_{o_{z_o}}(\omega)$ and $\Phi_{o_{y_o}}(\omega)$ and has been converted to frequency in cycles per second in place of the usual radians per second.

TABLE V

FYLON TRANSFER FUNCTIONS

$$Z'_o(i\ ) = \frac{-2257.414\left[(\omega^2-182.916)-i182.916g\right]\left[(\omega^2-616.9123)-i616.9123g\right]\left[(\omega^2-4004.1101)-i4004.1101g\right]}{\left[(\omega^2-184.3014)-i184.3014g\right]\left[(\omega^2-547.6283)-i547.6283g\right]\left[(\omega^2-2552.501)-i2552.501g\right]\left[(\omega^2-3959.248)-i3959.248g\right]}$$

$$Y'_o(i\ ) = \frac{-408.8757\omega^2\left[(\omega^2-160.0018)-i160.0018g\right]\left[(\omega^2-5455.8760)-i5455.8760g\right]}{\left[(\omega^2-184.3014)-i184.3014g\right]\left[(\omega^2-547.6283)-i547.6283g\right]\left[(\omega^2-2552.501)-i2552.501g\right]\left[(\omega^2-3959.248)-i3959.248g\right]}$$

$$Z'_i(i\ ) = \frac{-3561.771\left[(\omega^2-185.911)-i185.911g\right]\left[(\omega^2-583.861)-i583.861g\right]\left[(\omega^2-2638.2305)-i2638.2305g\right]}{\left[(\omega^2-184.3014)-i184.3014g\right]\left[(\omega^2-547.6283)-i547.6283g\right]\left[(\omega^2-2552.501)-i2552.501g\right]\left[(\omega^2-3959.248)-i3959.248g\right]}$$

$$Y'_o(i\ ) = \frac{1104.481\omega^2\left[(\omega^2-207.2201)-i207.2201g\right]\left[(\omega^2-2557.5046)-i2557.5046g\right]}{\left[(\omega^2-184.3014)-i184.3014g\right]\left[(\omega^2-547.6283)-i547.6283g\right]\left[(\omega^2-2552.501)-i2552.501g\right]\left[(\omega^2-3959.248)-i3959.248g\right]}$$

TABLE VI

CALCULATION OF OUTPUT POWER DENSITY SPECTRA

ω cps	$\Phi_i(\omega)$ g^2/cps	$\left\|Z_o'(i\omega)\right\|^2$	$\Phi_{o_{z_o}}(\omega)$ g^2/cps	$\left\|Y_o'(i\omega)\right\|^2$	$\Phi_{o_{y_o}}(\omega)$ g^2/cps
0	0	.991	0	0	0
0.10	12	1.001	12.012	0.000002	0
0.25	50	1.0033	50.165	0.000006	0.0003
0.35	100	1.0055	100.550	0.000008	0.0008
0.40	130	1.0068	130.884	0.000010	0.0013
0.45	145.5	1.0082	146.693	0.000011	0.0016
0.48	148	1.0094	149.391	0.000012	0.0018
0.504	145	1.0104	146.508	0.000012	0.0017
0.55	123	1.0124	124.525	0.000030	0.0037
0.60	99	1.0150	100.485	0.000050	0.0050
0.65	74	1.0179	75.325	0.000072	0.0053
0.70	61	1.0208	62.269	0.000090	0.0055
0.75	50	1.0240	51.200	0.000111	0.0056
0.80	40	1.0277	41.108	0.00013	0.0052
0.90	29	1.0355	30.030	0.000175	0.0051
0.95	22.5	1.0399	23.398	0.000195	0.0044
1.007	14	1.0453	14.634	0.000216	0.0030
1.05	7.1	1.0497	7.453	0.000189	0.0013
1.2	4.1	1.0660	4.371	0.000117	0.0005
1.424	2.0	1.0944	2.189	0.00005	0.0001
1.592	1.2	1.1171	1.341	0.001355	0.0016
1.750	1.0	1.135	1.135	0.0015	0.0015

TABLE VI (Continued)

ω cps	$\Phi_i(\omega)$ g^2/cps	$\lvert Z_o(i\omega)\rvert^2$	$\Phi_{o_{z_o}}(\omega)$ g^2/cps	$\lvert Y_o(i\omega)\rvert^2$	$\Phi_{o_{y_o}}$ g^2/cps
2.000	1.0	1.138	1.138	0.00038	0.0004
2.014	1.0	1.1378	1.138	0.000351	0.0004
2.075	0.8	1.0770	0.862	0.0024	0.0019
2.105	0.6	1.0264	0.616	0.0132	0.0079
2.135	0.6	1.0278	0.617	0.0768	0.0461
2.141	0.65	1.0661	0.693	0.1123	0.0730
2.147	0.7	1.1312	0.792	0.1630	0.1141
2.154	0.80	1.25691	1.006	0.2594	0.2075
2.160	0.9	1.3637	1.227	0.2952	0.2657
2.172	1.0	1.5787	1.579	0.3201	0.3201
2.176	1.1	1.6362	1.800	0.3904	0.4294
2.182	1.15	1.6772	1.929	0.3681	0.4233
2.188	1.2	1.6935	2.032	0.3351	0.4021
2.194	1.25	1.7243	2.155	0.3046	0.3808
2.222	1.50	1.6304	2.446	0.1757	0.2636
2.251	1.3	1.5741	2.046	0.1229	0.1598
2.291	0.8	1.5329	1.226	0.0891	0.0713
2.4	0.1	1.520	0.152	0.0781	0.0078
2.45	0.1	1.530	0.153	0.0781	0.0078
2.516	0.2	1.5573	0.311	0.0813	0.0163
2.6	1.0	1.600	1.600	0.0911	0.0911
2.7	1.7	1.68	2.856	0.115	0.1955
2.758	1.3	1.7235	2.241	0.1411	0.1834

TABLE VI (Continued)

ω cps	$\Phi_i(\omega)$ g^2/cps	$\lvert Z_o(i\omega)\rvert^2$	$\Phi_{o_{z_o}}(\omega)$ g^2/cps	$\lvert Y_o(i\omega)\rvert^2$	$\Phi_{o_{y_o}}(\omega)$ g^2/cps
2.978	0.7	1.9905	1.393	0.2829	0.1980
3.184	0.6	2.4550	1.473	0.6570	0.3942
3.376	0.5	3.4441	1.722	1.9226	0.9613
3.664	0.3	17.5080	5.252	48.5578	14.5673
3.698	0.3	24.7977	7.439	88.8778	26.663
3.716	0.3	26.0195	7.806	105.6358	31.691
3.722	0.3	25.3142	7.594	108.0663	32.420
3.726	0.3	24.6932	7.408	108.0980	32.429
3.727	0.3	23.6623	7.099	108.1011	32.430
3.729	0.3	23.9123	7.174	107.3784	32.214
3.732	0.3	22.9585	6.888	105.8416	31.752
3.766	0.3	11.2246	3.367	70.1983	21.059
3.800	0.2	4.4197	0.884	40.3848	8.077
3.833	0.2	1.7496	0.350	24.8528	4.971
3.848	0.2	1.0920	0.218	21.1594	4.232
3.866	0.2	0.7056	0.141	16.6669	3.333
3.898	0.15	0.2879	0.043	11.9858	1.798
3.931	0.15	0.1286	0.019	9.0978	1.365
3.955	0.1	0.0920	0.009	7.7033	0.7703
3.963	0	0.0796	0	7.1831	0
5.033	0	1.5849	0	0.8110	0
8.041	0	850.990	0	198.747	0

The power density spectra of the responses are plotted in Fig. 12 and Fig. 13. Similar results could be calculated for the inboard store, however, this is not essential for the purpose of this investigation.

It is noted that the spectrum of vertical acceleration response at the center of gravity of the outboard store as shown in Fig. 12 is quite similar to the input of Fig. 11, except for a small build-up in $\Phi_{o_{z_o}}(\omega)$ above 2.0 cycles per second where very little input amplitude exists. The mean-square acceleration for each spectrum has been determined by equation (57) and from this, the standard deviation, σ. Each of these is noted on the power density spectrum plots. The vertical output σ is 2.6 percent greater than the input σ.

The spectrum of induced lateral acceleration response at the center of gravity of the outboard store, shown in Fig. 13, is concentrated primarily at 3.73 cycles per second, a natural frequency for the pylon and store combination. Although there is very little input amplitude in this frequency range, the resonance produces a comparatively large response amplitude. The associated mean-square acceleration for the spectrum, $\phi_{o_{y_o}}(0)$, and standard deviation, σ, are noted on Fig. 13.

3.4 Evaluation of Results

A display of the significance of the results is obtained by determining the number of times per hour that given vertical and lateral load factors or accelerations at the center of gravity of the outboard store are exceeded, as indicated by:

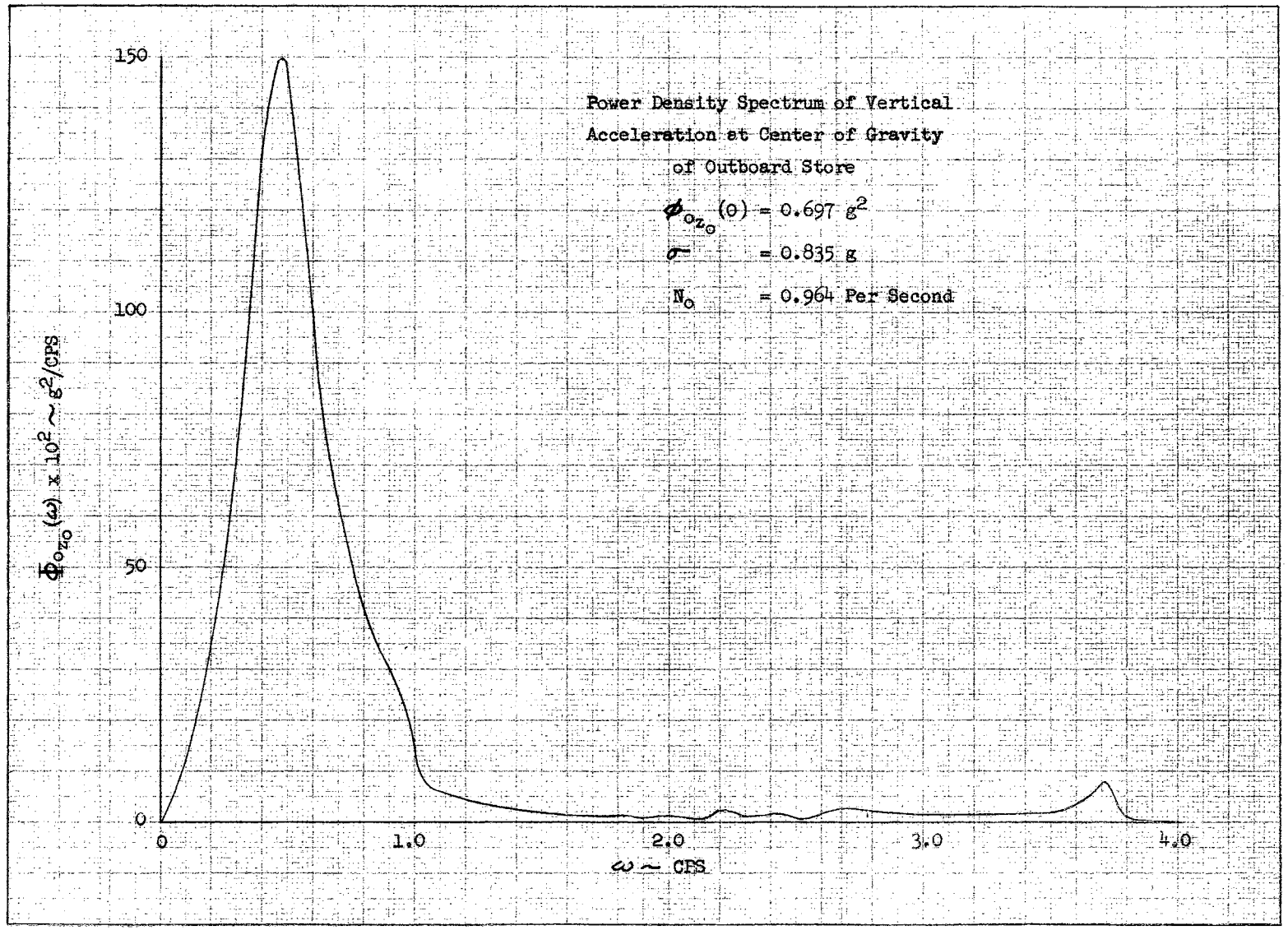

Fig. 12 Vertical Output Power Density Spectrum

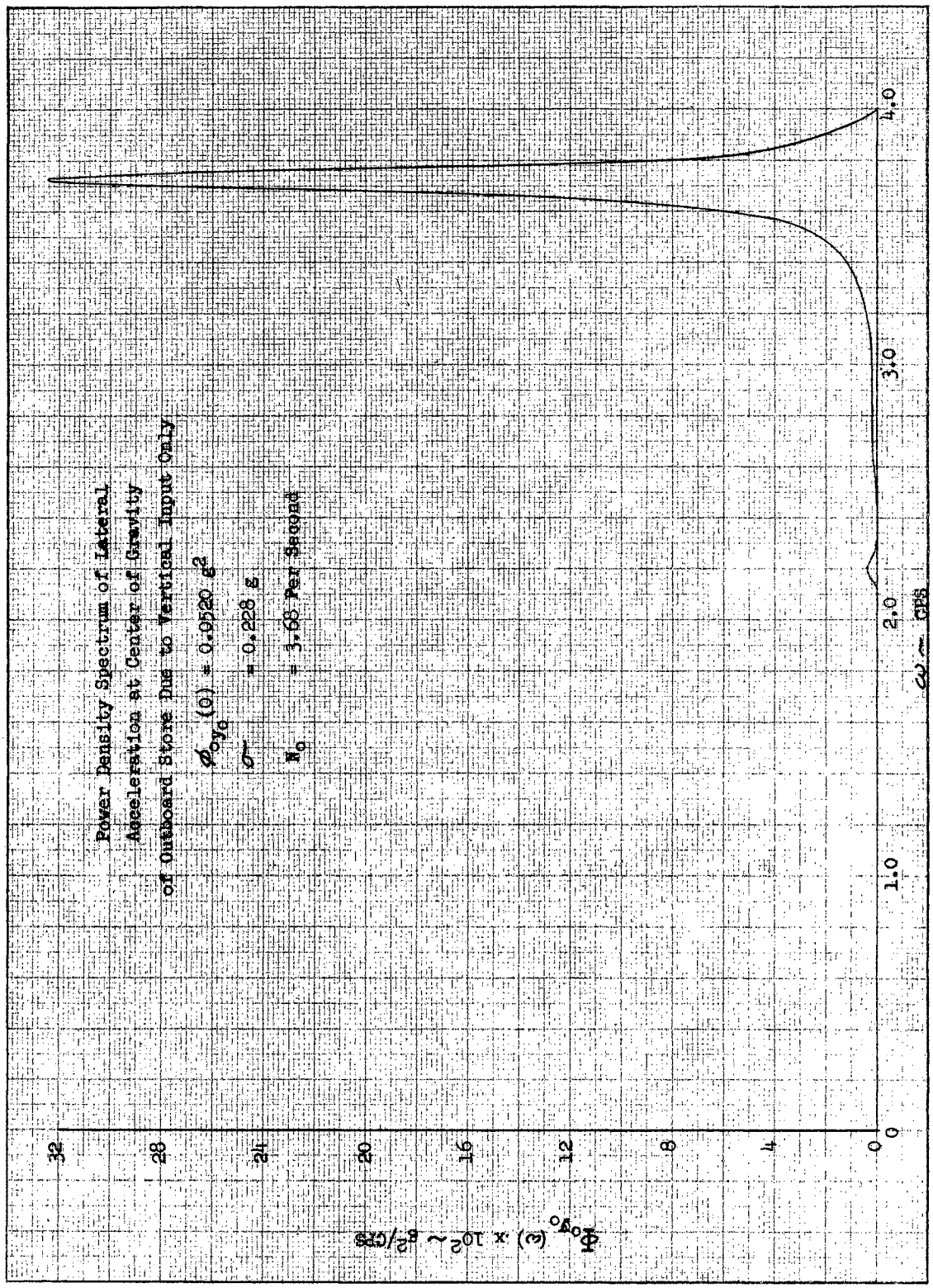

Fig. 13 Lateral Output Power Density Spectrum

a. The input power density spectrum if it were assumed applicable to the center of gravity of the store.

b. The output power density spectra.

This is accomplished by the use of equation (62) multiplied by 3600 seconds/hour:

$$N'(\Delta n) = 3600\, N_o e^{\frac{-\Delta n^2}{2\sigma_{\Delta n}}}, \qquad (95)$$

where

$$N_o = \left[\frac{\int_o^\infty \omega^2 \Phi_o(\omega)\, d\omega}{\int_o^\infty \Phi_o(\omega)\, d\omega}\right]^{1/2}$$ for ω in terms of cycles per second

Δn = the load factor or acceleration of concern.

$N'(\Delta n)$ = average number of maximum load factors or accelerations per hour exceeding Δn

The calculated value of N_o for each power density spectrum is shown on Fig. 11, 12, and 13.

The resulting excedence curves for incremental vertical load factor only are plotted on Fig. 14. This figure shows both the load factor excedences indicated by the basic input and the load factor excedences indicated by the vertical output at the center of gravity of the outboard store.

The resulting excedence curve for lateral load factor at the center of gravity of the outboard store is shown in Fig. 15. The basic vertical input, without consideration of the pylon flexibility and the resulting transfer functions, would, of course, indicate no occurances of lateral load factor.

The lateral load factor output may be converted to equivalent incremental vertical load factor by recourse to the

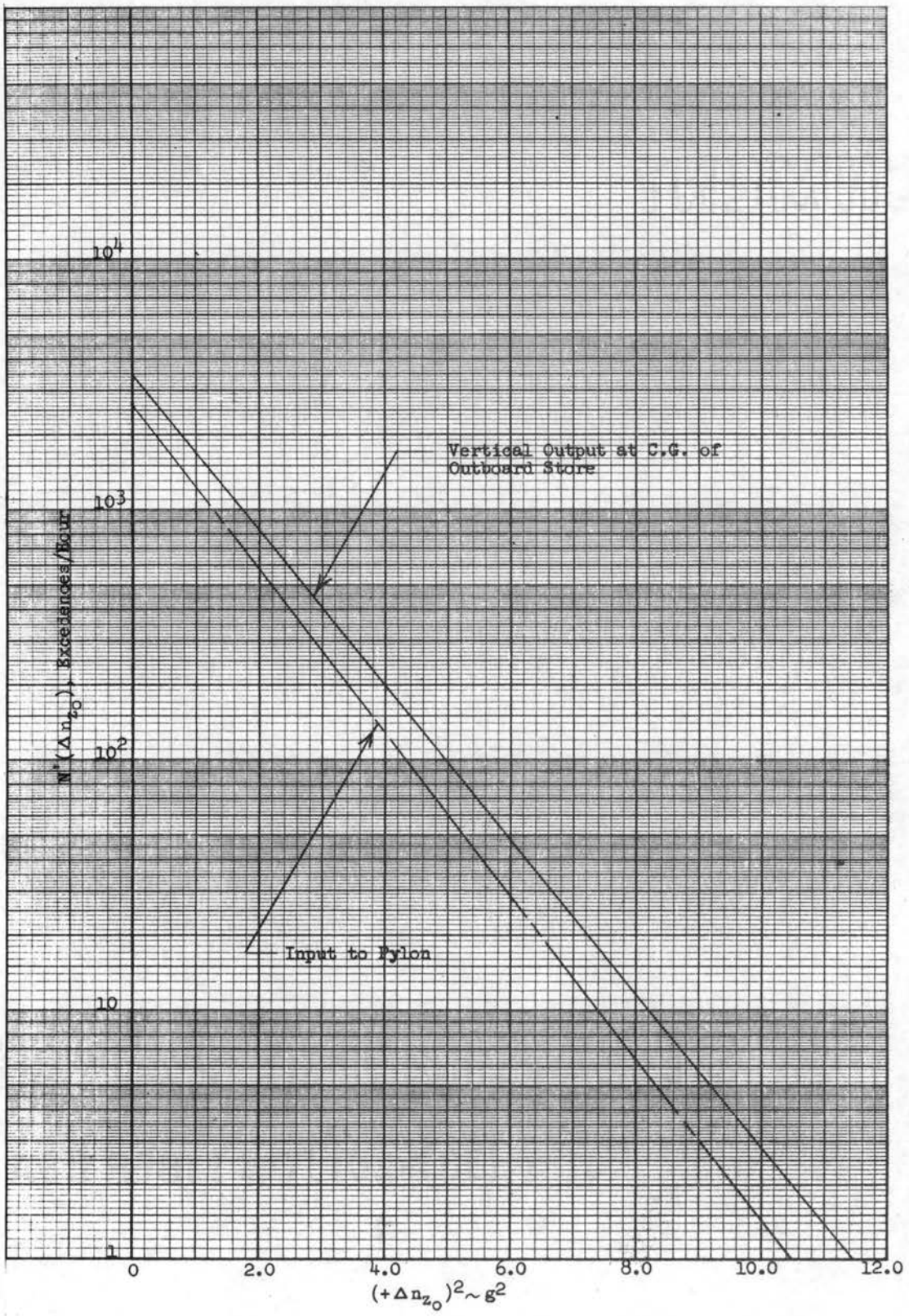

Fig. 14 - Incremental Vertical Acceleration Excedences

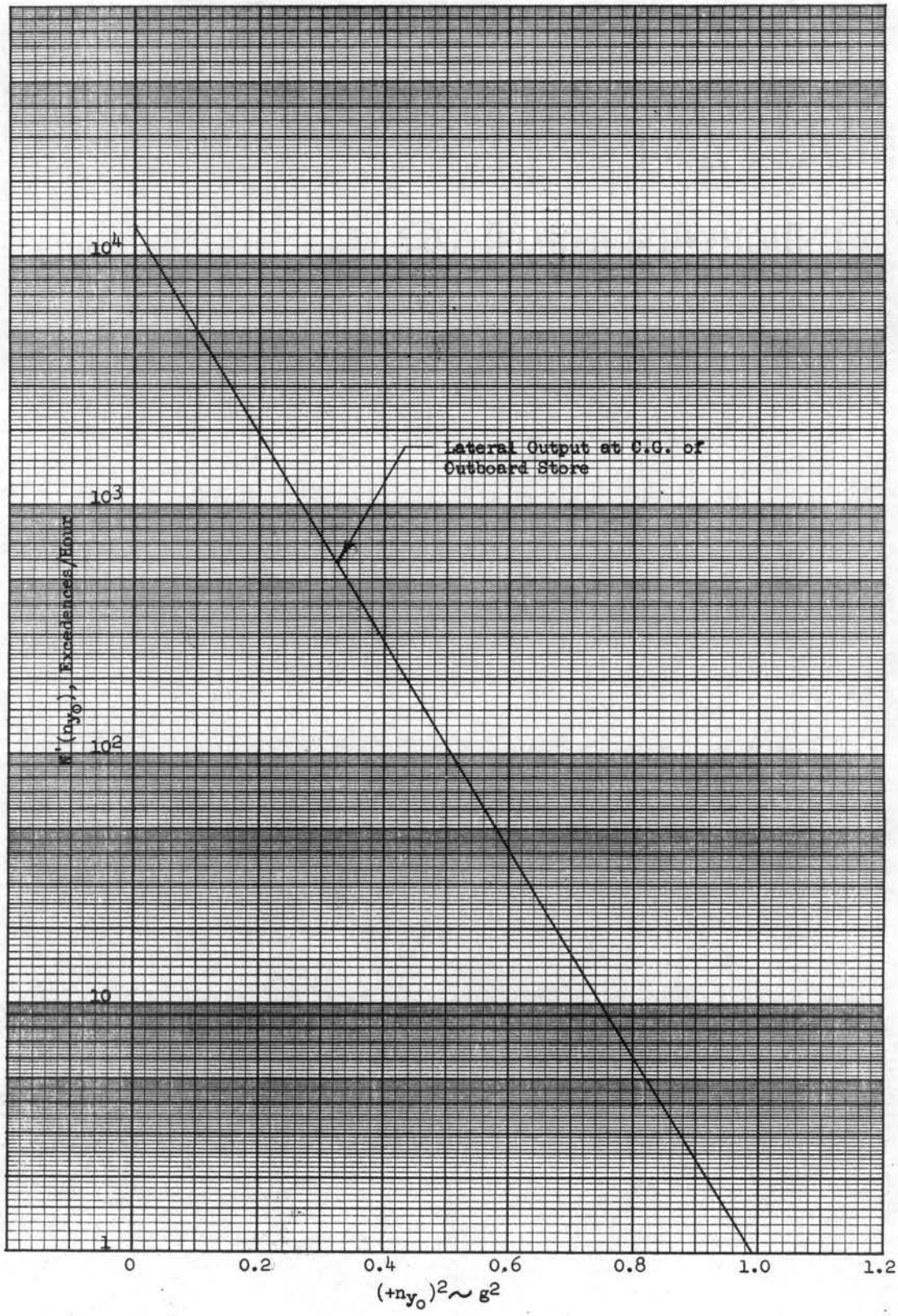

Fig. 15 - Lateral Acceleration Excedences

initial statement that a lateral load factor of 1.0g produces a critical stress equivalent to that produced by a vertical load factor of 2.75g. This conversion results in the curve of Fig. 16.

The total equivalent combined output, the vertical load factor output only, and the vertical load factor input excedences are all shown for summary purposes on Fig. 17.

These observations are made:

a. The incremental vertical load factor which is input at the pylon to wing attachment no more frequently than once an hour is 3.24g whereas the output at the c.g. of the outboard store occuring with the same frequency is 3.37g, an increase of 4 percent which is rather small and not of particular structural significance.

b. The cyclic loading, which is of prime concern from a structural fatigue standpoint, has been developed from Fig. 17 and is shown in Table VII. This table shows the number of applications per hour of average incremental vertical load factors as developed directly from the input to the pylon and also as developed from the total equivalent vertical output at the c.g. of the outboard store. The total equivalent vertical output indicates approximately an 800 percent increase over the input in the number of load cycles predicted at the lower load factors, diminishing to approximately a 70 percent increase at the higher load factors. The large increase at the lower load factors is primarily due to the induced lateral effects.

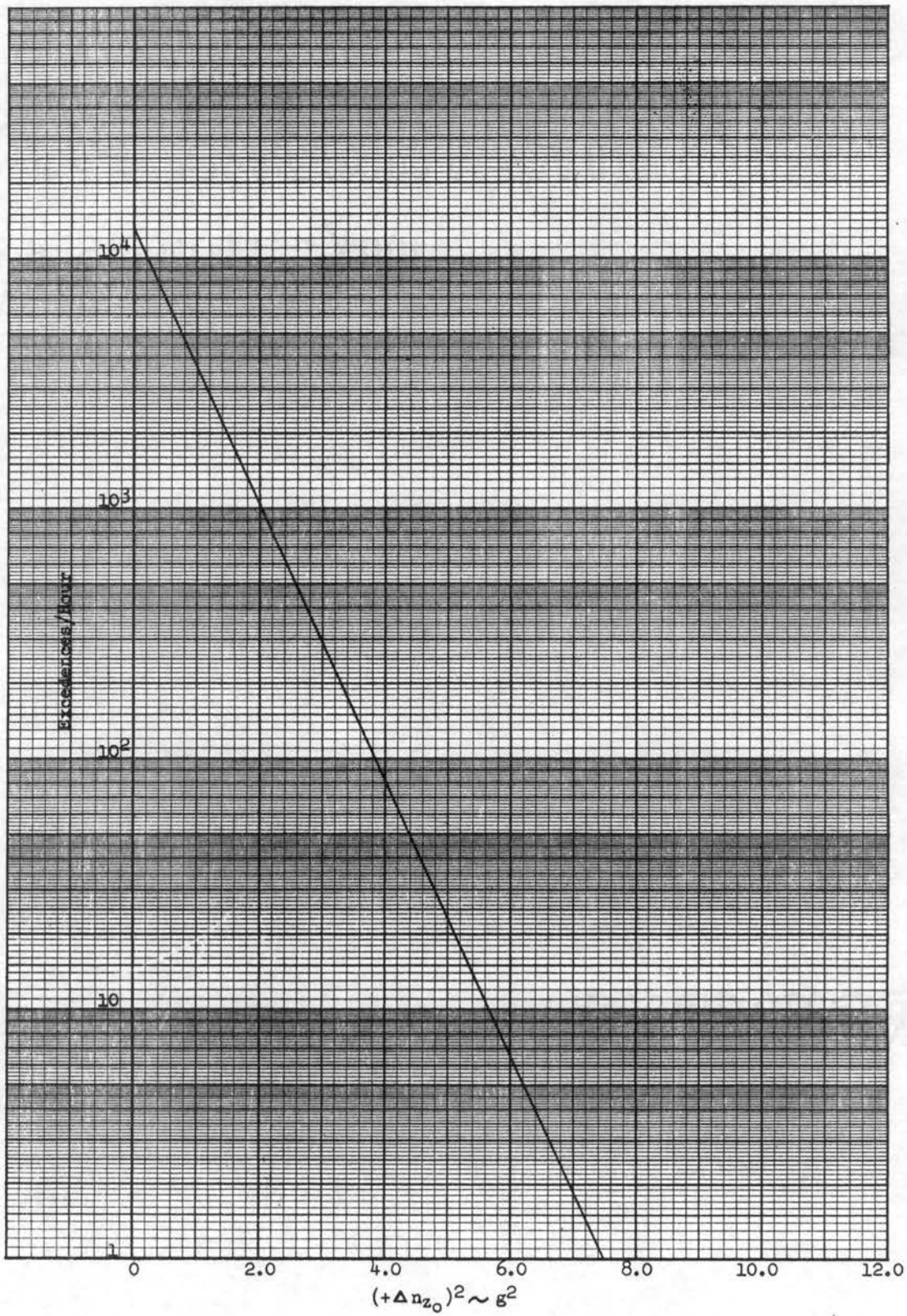

Fig. 16 - Equivalent Incremental Vertical Acceleration Excedences from Lateral Response

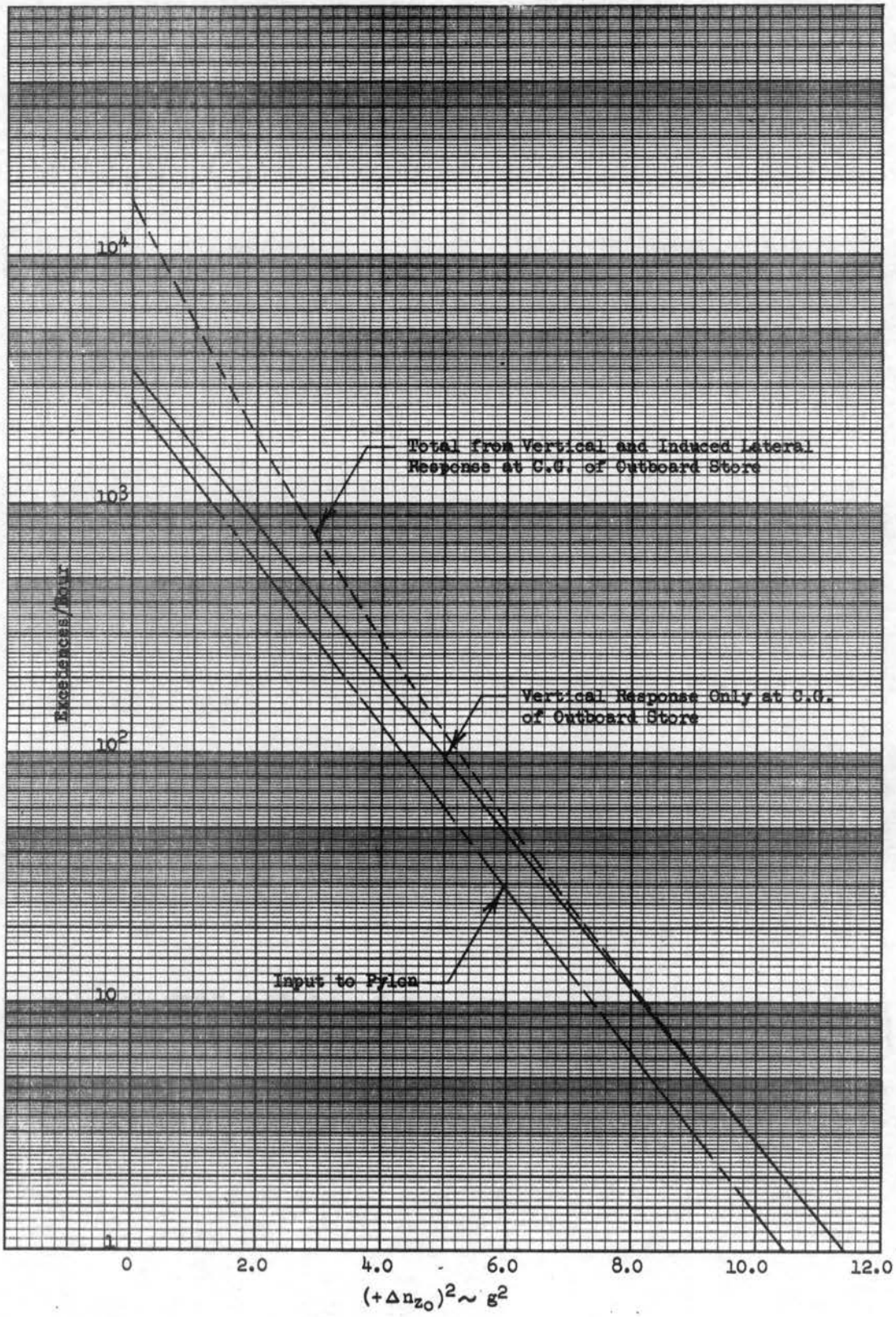

Fig. 17 - Total Equivalent Incremental Vertical Excedences from Vertical and Lateral Response

TABLE VII

CYCLIC LOAD PREDICTION

Δn_z g's	Input to Pylon Excedences/Hr.	Input to Pylon Cycles/Hr.	Vertical Output Only Excedences/Hr.	Vertical Output Equivalence of Lateral Output Excedences/Hr.	Total Equivalent Vertical Output Excedences/Hr.	Total Equivalent Vertical Output Cycles/Hr.
0	2640		3470	13,250	16,720	
		470				4270
0.5	2170		2850	9,600	12,450	
		920				7050
1.0	1250		1690	3,710	5,400	
		770				3960
1.5	480		680	760	1,440	
		350				1161
2.0	130		197	82	279	
		106				236
2.5	24		38.5	4.6	43	
		21				38
3.0	3		5.4		5	

c. This increase in cyclic loading would be reflected in a significantly shorter "failure free" flight life for the pylon structure than would be anticipated from a consideration of the basic input cyclic loading alone.

Although these observations apply to the specific problem, it would appear that the admittance or transfer functions of any pylon or store supporting structure can significantly alter the predicted cyclic inertia loading if natural frequencies for the system exist anywhere within the frequency range covered by the input power density spectrum. In general, this will cover the frequency range from zero to ten cycles per second, for an input developed by atmospheric turbulence.

A complete evaluation of the cyclic stresses induced in the pylon due to combined vertical and induced lateral loading revealed in this investigation should be based on calculations of the associated pylon mode shapes at the critical natural frequency. This would provide a guide in combining the proper simultaneous effects.

A prediction of the <u>total</u> cyclic fatigue loading history for any pylon must consider both vertical and lateral gust inputs. Further, these inputs must obviously cover the anticipated flight environment, as discussed in Chapter II, rather than just one rather severe gust input as used in this investigation.

The demonstrated importance associated with a structural resonance point, along with the possibility for the interaction of vibration modes of pylon, wing, and other structure, would indicate that in all cases, final evaluation of the

cyclic loading on a pylon and store must come from flight test. Design and development testing come long before flight, however, and must rely on analytics such as applied in this investigation.

CHAPTER IV

SUMMARY AND CONCLUSIONS

The determination of aircraft gust loads by the use of power density spectra is discussed. These methods are applied to investigate the structural significance of considering the transfer functions of a hypothetical wing mounted pylon and supported store combination to obtain the acceleration output at the store center of gravity from a known acceleration input at the pylon to wing attachment points.

The basic fundamentals essential for the understanding and proper application of power density spectra are covered in detail. The published power spectral density analysis methods for the prediction of aircraft gust loads are set forth and discussed with reference to the basic fundamentals.

The investigation of the wing mounted pylon and supported store demonstrates that the transfer functions of a pylon supporting a high mass item can alter the power density spectrum of input acceleration to a degree which is important in evaluating the structural fatigue characteristics of the pylon. This is considered possible if the pylon and store combination have a natural frequency anywhere within the frequency range covered by the input power density spectra. In general, this would be from zero to ten cycles per second for an input developed by atmospheric turbulence.

It is observed in the example chosen for investigation, that the higher amplitude portion of the input power density spectrum, Fig. 11, is confined to the region of 2.0 cycles per second and below. The example pylon-store system resonant frequencies occur above 2.0 cycles per second where the input spectrum amplitude is quite small. This has minimized the influence that the pylon flexibility has on the cyclic loading due to this input; yet this influence has proven significant. It is therefore apparent that where practical, a pylon structure should be designed to avoid resonant frequencies which coincide with the high amplitude frequency ranges of all known input spectra.

A power spectral density analysis may be used as demonstrated herein to predict the frequency of occurance of cyclic fatigue loads from given input spectra. Further, as demonstrated, there may be several types of output responses resulting from a single input; for example, vertical and lateral acceleration outputs due to a vertical acceleration input.

The proper time coordination of these types of output response is important in structural fatigue testing but is not defined in the power density analysis. A study of pylon mode shapes at the critical natural frequencies could serve as a guide in combining the proper simultaneous effects.

BIBLIOGRAPHY

1. Newton, G. C., Jr., Gould, L. A., and Kaiser, J. F., Analytical Design of Linear Feedback Controls. New York: John Wiley and Sons, Inc., 1957

2. Cheng, David K., Analysis of Linear Systems. Reading, Mass.: Addison-Wesley Publishing Co., Inc., 1959

3. Truxal, John G., Automatic Feedback Control System Synthesis. New York: McGraw-Hill Book Co., Inc., 1955

4. MIL-S-5702 (USAF) Structural Criteria, Piloted Airplanes, Basic Flight Criteria. Military Specification, 14 December 1954

5. Clementson, Gerhardt C., An Investigation of the Power Spectral Density of Atmospheric Turbulence. Ph. D. Thesis, M.I.T., 1950

6. Press, Harry and Mazelsky, Bernard. A Study of the Application of Power-Spectral Methods of Generalized Harmonic Analysis to Gust Loads on Airplanes. National Advisory Committee for Aeronautics: Technical Note 2853, 1953

7. Press, H., Meadows, M. T., and Hadlock, I. A Reevaluation of Data on Atmospheric Turbulence and Airplane Gust Loads for application in Spectral Calculations. National Advisory Committee for Aeronautics: Technical Report 1272, 1956

8. Press, Harry and Steiner, Roy. An Approach to the Problem of Estimating Severe and Repeated Gust Loads for Missile Operations. National Advisoty Committee for Aeronautics: Technical Note 4332, 1958

9. Saunders, K. D., et al. Interim Report on the Technical Analysis of the B-66B Low Level Gust Study. Douglas Aircraft Co., Inc.: Report SM 23973, 1960

10. Rice, S. O., Mathematical Analysis of Random Noise, Parts I and II. Bell System Technical Journal, Vol. XXIII, no. 3, July 1944, pp. 282-332; Parts III and IV, Vol. XXIV, no. 1, Jan. 1945, pp. 46-156.

11. MIL-A-8866 (ASG) Airplane Strength and Rigidity Reliability Requirements, Repeated Loads, and Fatigue. Military Specification, 18 May 1960.

12. Scanlon, Robert H. and Rosenbaum, Robert. Introduction to the Study of Aircraft Vibration and Flutter. New York: The MacMillan Company, 1951.

13. Fung, Y. C., An introduction to the Theory of Aeroelasticity. New York: John Wiley and Sons, Inc., 1955

VITA

Lloyd Earl Jackson

Candidate for the Degree of

Master of Science

Thesis: POWER DENSITY SPECTRA AND THEIR APPLICATION IN THE DETERMINATION OF AIRCRAFT GUST LOADS

Major Field: Civil Engineering

Biographical:

Personal Data: Born on September 21, 1923 in Pittsburgh, Pennsylvania, the son of Lloyd E. and Hazel D. Jackson.

Education: Attended grade school in Los Angeles, California; Kansas City, Missouri; and Pittsburgh, Pennsylvania. Graduated from Topeka High School, Topeka, Kansas, in 1940. Received the Bachelor of Science degree from the University of Tulsa, Tulsa, Oklahoma, with a major in Aeronautical Engineering, in May 1949. Completed requirements for the Master of Science degree in August 1961.

Professional Experience: Served in the Army of the United States, Air Corps, from September 1942 to December 1945. Employed by Chance Vought Aircraft, Dallas, Texas, as an Aerodynamicist from August 1949 to June 1951. Employed by Douglas Aircraft Company, Tulsa, Oklahoma, from June 1951 to the present, specializing in aircraft and missile strength analysis.